APPENDIX A: DESCRIPTION OF INDIVIDUAL CCSNE ENVIRONMENTS

A brief description of the immediate environment of each ccSNe in its host galaxy is presented, together with ground-based net Hα and continuum images on a (projected) scale of 1×1 kpc (2×2 kpc or 4×4 kpc in some cases).

A1 SN 1923A in M 83

SN 1923A (II-P) was discovered in May 1923, 2.1′ (0.33 R_{25}) NE from the centre of M 83 (NGC 5236, Pennington et al. 1982). The low inclination of M 83 implies negligible projection effects, so this corresponds to 3.0 kpc for the adoped 4.9 Mpc distance to M 83 (1″ closely approximates to 25 pc). As illustrated in Fig. A1, the SN position is immediately to the south of a bright, extended, star-forming region in our VLT/FORS2 imaging from June 2002, # 59 from the H II region catalogue of Rumstay & Kaufman (1983). A giant H II region within the complex lies 4″ (100 pc) to the N of the SN position, although extended emission extends significantly closer in our VLT/FORS2 imaging. The luminosity of the H II region is comparable to N66 (SMC), for which we measure 1.7×10^{38} (7.8×10^{38}) erg s^{-1} using a 1″ (4″) radius aperture. HST WFC3 imaging (GO 11360, PI R.W. O'Connell) using the F657N filter provides a higher spatial view of the region, and reveals several point sources within the error circle of the SN position, plus a faint arc coincident with the SN that extends further to the SW. A more extended star forming region, #79 from Rumstay & Kaufman (1983), lies ∼23″ (0.55 kpc) to the W, at the edge of Fig. A1.

A2 SN 1964H in NGC 7292

This type II supernova occurred 29″ to the SW of the nucleus of NGC 7292 (Porter 1993), corresponding to a deprojected distance of 32″ (0.51 R_{25}) or 2.0 kpc for the adopted distance of 12.9 Mpc to NGC 7292. Calibrated JKT imaging of NGC 7292 from Jul 2000 (James et al. 2004) has been supplemented by INT/WFC imaging from Jul 1999. The latter are presented in Fig. A2, indicating that the SN location is devoid of nebular emission, with the closest Orion-like H II region to the SN offset 5″ to the NW, a deprojected distance of 350 pc away. Brighter, giant H II regions lie 7″ (0.5 kpc) to the W and 8″ (0.55 kpc) to the SW, with Hα-derived luminosities of 1.3×10^{38} erg s^{-1} and 4.8×10^{38} erg s^{-1}, respectively. From inspection of HST WFPC2 imaging with the F300W filter (GO 8632, PI M.Giavalisco), no source is detected either at the position of the SN or the closest H II region.

A3 SN 1968D in NGC 6946

SN 1968D (II) was discovered in Feb 1968, in a region of NGC 6946 lacking nebular emission, 0.8′ (0.14 R_{25}) NE of its centre (van Dyk et al. 1994). The low inclination of NGC 6946 implies projection effects are negligible, so 1″ = 35 pc for the adopted distance of 7 Mpc. From our Gemini/GMOS imaging obtained in Aug 2009, the nearest major star forming region is located SSE of the SN position (van Dyk et al. 1996), Figure A3 shows that this comprises diffuse emission extending over 6″ (200 pc) plus two marginally extended sources. Of these, the closest to the SN location lies 4″.5 (150 pc) away, and has a luminosity somewhat in excess of Orion, according to our Gemini GMOS imaging.

Additional isolated Orion-like H II regions are offset 6–7″ (200-230 pc) to the WNW and WSW, while brighter, extended H II regions lie 12″ (400 pc) to the NNE and 17″ (550 pc) to the NNW, with luminosities of 7×10^{37} erg s^{-1} and 1.4×10^{38} erg s^{-1}, respectively.

From inspection of HST/WFPC2 F547M and F656N imaging (GO 8591, PI Richstone) neither a star cluster nor nebular emission are identified at the SN position. Isolated, moderately extended sources are responsible for the nearby Hα emission, while the brighter regions to the NNE and NNW are multiple.

A4 SN 1968L in M 83

This type II-P supernova was discovered in July 1968, and occurred within the nuclear starburst of M 83 (van Dyk et al. 1996). As for SN 1923A, the low inclination of M 83 implies negligible projection effects, such that 1″ approximates to 25 pc at 4.9 Mpc. Figure A4 shows that nebular emission is extremely strong at the position of the SN, albeit offset from the peak Hα emission, which lies to the N and E. At the spatial resolution (FWHM ∼ 0″.9 or 20 pc) of our VLT/FORS2 imaging from Jun 2002, the closest H II region is located 1″ (25 pc) to the E, and has a luminosity comparable to the Carina Nebula. Brighter giant H II regions lie 1″.5 (40 pc) to the SW and 2″ (50 pc) to the WNW, while a pair of exceptionally bright knots 4″ (100 pc) to the N, coincident with clusters #23, #24 and #27 from Harris et al. (2001), have a combined luminosity of 1.2×10^{40} erg s^{-1} (similar to 30 Doradus).

From an inspection of the narrow-band continuum image, SN 1968L is not spatially coincident with a bright cluster. This is confirmed from inspection of HST WFPC2/F547M (GO 8234, PI D.Calzetti) and HST WCF3/F555W imaging (GO 11360, PI R.W. O'Connell), while WFC3/F657N imaging reveals solely diffuse emission at the SN position. The nebular emission to the E of SN 1968L is spatially extended, while a single compact source is responsible for the giant H II region to the NW. The nearest continuum sources to the SN location are clusters #13 and #15 from Harris et al. (2001) which are coincident with the giant H II region 1″.5 to the SW of the supernova position.

A5 SN 1970G in M 101

SN 1970G (II-L) was discovered in Aug 1970, and occurred close to a very bright, spatially extended H II region NGC 5455 (Allen et al. 1976; Cowan et al. 1991), 6.6′ (0.46 R_{25}) SW of the nucleus of M 101 (NGC 5457). Owing to the low inclination of M 101, there are no projection effects, so this corresponds to a distance of 13.5 kpc for the adopted 6.9 Mpc distance to M 101 (3″ corresponds to 100 pc). Due to the low resolution of the Hoopes et al. (2001) imaging, we employ higher spatial resolution INT/WFC imaging from Jun 2006 (FWHM∼1″.1) to assess the detailed nebular morphology. From Fig. A5, the SN position is located at the periphery of NGC 5455, with the peak Hα and continuum emission (# 416 from Hodge et al. 1990) located 5″ (170 pc) to the SE of the SN location. The Hα-derived luminosity of this region is 2×10^{40} erg s^{-1}, comparable to 30 Doradus, based on the Hoopes et al. (2001) imaging. The INT/WFC imaging reveals a faint continuum source within ∼1″ of the position of SN 1970G (right panel of Fig. A5. Higher resolution HST WFPC2 imaging using the F606W filter (GO 6713, PI W.B. Sparks) suggests that the SN is not coincident with nebular emission, with the nearest bright continuum source offset E by 1″.6.

A6 SN 1980K in NGC 6946

This type II-L supernova, discovered in Oct 1980, occurred in the outer disk of NGC 6946, 5′.45 to the SE of the nucleus, which corresponds to a deprojected distance of 5′.7 (0.99 R_{25}) or 11.5kpc for the 7 Mpc distance to NGC 6946. Based on the radio SN position from Weiler et al. (1992), it fell beyond the field-of-view of our Gemini GMOS imaging, so instead we employ the KPNO 2.1m imaging from Mar 2001 (Kennicutt et al. 2003). Fig. A6 shows that there is no significant Hα emission close to the position of the SN. Extended H II regions lie 50″ (1.75 kpc) W, 60″ (2.1 kpc) WNW and 55–65″ (1.9–2.3 kpc) NE, with luminosities of 2×10^{37} erg s^{-1}, 4×10^{37} erg s^{-1} and 5×10^{37} erg s^{-1}, respectively. SN 1980K is seen as a point source in HST/WFPC2 F606W imaging (GO 11229, PI M. Meixner), with a second, visually fainter point source 0″.5 (20 pc) to its E (Sugerman et al. 2012).

A7 SN 1983N in M 83

The type Ib SN 1983N was discovered in July 1983 (Wamsteker 1983), and occurred 3′ SW of the nucleus of M 83 (NGC 5236), corresponding to a deprojected distance of 3′.1 (0.48 R_{25}) or 4.4 kpc for the adopted distance of 4.9 Mpc to M 83. Based upon the radio position of Sramek et al. (1983) this is close to a complex of star formation to the E, SW and very bright nebular emission to the SE. Clocchiatti et al. (1996) enable relative astrometry from our Jun 2002 VLT/FORS2 imaging. Figure A7 illustrates that an extended H II region, #222 from the catalogue of Rumstay & Kaufman (1983), lies 1″ (25 pc) to the east of the SN, which has a luminosity intermediate between the Orion and Rosette nebulae. An arc of nebular emission lies 9″ (220 pc) to the SW of SN 1983N, alias # 234 from Rumstay & Kaufman (1983). This has an integrated luminosity of 1.6×10^{38} erg s^{-1} (3″ radius) while a giant H II region, #220 from Rumstay & Kaufman (1983), peaks 9″ (220 pc) to the SE and and has a luminosity comparable to N66 (SMC). Broad band HST/STIS imaging (GO 9148, PI P. Garnavich) reveals several faint sources consistent with the SN error box, with brighter clusters coincident peak emission from the H II regions to the E, SW and SE.

A8 SN 1985F in NGC 4618

This type Ib/c supernova was discovered in Feb 1985 (Filippenko & Sargent 1985, 1986, Modjaz, priv. comm.), and is spatially coincident with a bright H II region and cluster, 10″ away from the centre of NGC 4618 (Filippenko et al. 1986), as shown in Fig. A8. Based upon the HyperLeda inclination and PA of the major axis of NGC 4618 this corresponds to a deprojected offset of 12″ (0.1 R_{25}) or 0.5 kpc for the adopted distance of 9.2 Mpc to NGC 4618. Using the SN position of Filippenko & Sargent (1986), the 2.3m Bok imaging of NGC 4618 from Apr 2001 (Kennicutt et al. 2008) reveals that the Hα-derived luminosity of this (extended) region is N66-like, and is comparable to that of a neighbouring H II region, 4″ to the SW of SN 1985F, a deprojected distance of 220 pc away. HST/WFPC2 imaging using the F606W filter (GO 5446, PI Illingworth) confirms that the SN is coincident with an extended source, while each of the ground-based continuum sources to the W and SW in spatially resolved into two primary extended clusters.

A9 SN 1986L in NGC 1559

SN 1986L (II-L) was discovered in NGC 1559 in Oct 1986 (Evans et al. 1986). Figure A9 presents net Hα VLT/FORS1 imaging obtained in Aug 2005 and reveals that the SN lies in an extended region of nebular emission, which extends north from a giant H II region several arcsec to the SW. This complex is 45″ west of the centre of NGC 1559, and corresponds to a deprojected offset of 1′ (0.55 R_{25}) based on the HyperLeda inclination and major axis PA, equivalent to 3.5 kpc for the 12.6 Mpc distance to NGC 1559 (100 pc corresponds to 1″.3). The nebular flux at the SN position is relatively faint, based upon the astrometry of McNaught & Waldron (1986). H II regions are located 2″ (150 pc) to the NNE and 3″ (230 pc) to the NW with luminosities of 8×10^{37} erg s^{-1} and 1.2×10^{38} erg s^{-1}, respectively. In addition, a giant H II region ∼3″ (230 pc) to the SW of SN 1986L has a luminosity comparable to the Carina Nebula. Unfortunately, SN 1986L occurred outside the field of view of HST/WFPC2 imaging (GO 9042, PI S.J. Smartt).

A10 SN 1987A in LMC

SN 1987A, the best studied supernova of the modern era, lies in the periphery of the 30 Doradus (Tarantula Nebula) region of the LMC. Hα imaging from the Nikon Survey Camera (M.S. Bessell, priv. comm.) and MCELS (Smith et al. 2000) indicates faint nebular emission at the position of the SN. In Figure A10, we present the lower spatial resolution Parking Lot Camera images (Kennicutt et al. 1995), 70″ or 17 pc at the 50 kpc LMC distance. Nebular emission is present at the SN site, although it is relatively faint, and would not necessarily be detected in ground-based imaging of other ccSNe in our survey. Still, SN 1987A is is close proximity to a pair of bright knots of nebular emission 2–3′ (∼40 pc) to the NW, with an integrated luminosity of 6×10^{37} erg s^{-1} (2′ radius aperture), as measured from Nikon continuum-subtracted imaging, calibrated via Kennicutt et al. (1995). The centre of 30 Doradus lies 20′ (300 pc) to the NE, with an integrated luminosity of 6×10^{39} erg s^{-1} (10.5′ radius aperture). Panagia et al. (2000) discuss the faint cluster coincident with SN 1987A, but again this would not be detected via ground-based imaging of SN beyond the Local Group.

A11 SN 1992ba in NGC 2082

This type II supernova was discovered by R. Evans in NGC 2082 in late Sep 1992 (Evans & Phillips 1992). SN 1992ba occurred 26″ to the W of the nucleus of NGC 2082, which deprojects to 29″ (0.5 R_{25}) based on the low inclination from HyperLeda, plus an adopted PA=0.This corresponds to a galactocentric distance of 1.9 kpc for the 13.1 Mpc distance to NGC 2082. We do not have access to calibrated Hα imaging, so we have inspected archival R-band imaging from Oct 1992 (AAT Prime Focus) and Apr 2000 (3.5m NTT/EMMI). The latter are reveal continuum sources 2″ NW and 2″.5 SE, with a brighter source 3″.5 SE of SN 1992ba. Schmidt et al. (1994) note that this supernova occurred in, or near, a bright H II region.

A12 SN 1993J in M 81

This well-studied type IIb supernova was discovered in March 1993 (Ripero et al. 1993), and occurred 2′.8 SSW of the nucleus of M 81 (NGC 3031). The HyperLeda inclination of M 81 is high (62.7° so this position corresponds to a deprojected offset of 4′.4 (0.32 R_{25}), equivalent to a distance of 4.6 kpc for the 3.65 Mpc distance to

M 81. From the KPNO 2.1m imaging from Mar 2001 (Kennicutt et al. 2003), shown in Fig. A11, SN 1993J is spatially coincident with a faint nebular emission, likely arising from the SNR itself. A brighter, Orion-like region lies 21″ to the NE, or a deprojected distance of 580 pc. An extended H II region, with a Hα+[N II] flux of 4×10^{-14} erg s^{-1} cm^{-2} lies 38″ (1.0 kpc deprojected) to the NW. The blue supergiant companion to the red supergiant progenitor is detected in late-time spectroscopy (Maund et al. 2004) and spectroscopy (Maund & Smartt 2009), the latter based upon extensive HST ACS and WFPC2 imaging.

A13 SN 1994I in M 51a

This type Ic supernova occurred close to the nucleus of M 51a in Apr 1994 (Puckett et al. 1994), 18″ to its SE. The low inclination of 32.6° for M 51a implies negligible projection effects, so this corresponds to a distance of 0.8 kpc (0.06 R_{25}) for the adopted distance of 8.39 Mpc. Based on radio-derived coordinates from Rupen et al. (1994), Fig. A12 illustrates that SN 1994I lies within a large region of diffuse nebular emission. The closest identifiable source is a giant H II region 2″ (80 pc) to the W in the KPNO 2.1m imaging from Mar 2001 (Kennicutt et al. 2003). Brighter sources lie 9″ (0.38 kpc) SW and 13″ (0.55 kpc) W. SN 2004I does not appear to coincide with a bright star cluster in the KPNO 2.1m R-band imaging, although identification is severely hindered by diffuse emission and the moderate spatial resolution of the ground-based images. We have therefore inspected archival Hubble Space Telescope ACS/WFC (GO 10452, PI S. Beckwith) images obtained with the F555W and F658N (Hα+[N II]) filters (e.g. Chandar et al. 2011), which confirm no bright cluster is spatially coincident with SN 1994I.

A14 SN 1995V in NGC 1087

This type II-P supernova was discovered in Aug 1995 (Evans et al. 1995), and occurred 24″ E of the nucleus of NGC 1087 (Balam 1995). This corresponds to a deprojected offset of 40″ (0.36 R_{25}) or 2.8 kpc for the adopted distance of 14.4 Mpc to NGC 1087. Fig. A13 shows JKT Hα imaging from Jan 2000 (James et al. 2004). Although seeing conditions were poor (FWHM∼3″.5), SN 1995V does not appear to be coincident with nebular emission, with the nearest identifiable H II region (and bright cluster) located 5″ (0.6 kpc) to the SW.

A15 SN 1995X in UGC 12160

The type II supernova SN 1995X was discovered in UGC 12160 in Aug 1995 (Mueller et al. 1995). We do not have access to calibrated Hα imaging of UGC 12160, although Mueller et al. (1995) report narrow Hα emission from a H II region superimposed upon an early SN spectrum. The SN occurred 22″ NW of the centre of UGC 12160 (Sicoli et al. 1995), which corresponds to a deprojected distance of 26″ (0.42 R_{25}) or 1.8 kpc for the adopted distance of 14.4 Mpc to UGC 12160. At this location, Anderson et al. (2012) report a NCR pixel value of 0.903 from Liverpool Telescope RATCam imaging, indicating it occurred close to the peak of Hα emission from the host.

A16 SN 1996cr in Circinus

This type IIn supernova was discovered in Mar 1996, although was originally identified as an X-ray source (Bauer 2007). It occurred 24″ to the S of the nucleus of Circinus (ESO 097-G13), corresponding to a deprojected offset 37″ (0.18 R_{25}) or 0.75 kpc for a 4.21 Mpc distance to Circinus. This galaxy suffers extensive foreground extinction ($A_B \sim 2$ mag) due to its low galactic latitude ($b = -3.8°$). Hα imaging from Apr 2002 using the CTIO 0.9m (Kennicutt et al. 2008) is presented in Fig. A14. This reveals faint nebular emission at the position of SN 1996cr, as discssed by Bauer (2007), which connects to a bright H II region, 3″ to its SE, a deprojected distance of 100 pc away. A starburst ring of H II regions surrounds the (type 2 Seyfert) nucleus of Circinus (Marconi et al. 1994), the most southerly component of which lies 15″ (0.5 kpc) NNW of SN 1996cr. No cluster is apparent at the location of the SN, although the CTIO imaging was obtained during poor seeing conditions (FWHM∼3″.5). We have therefore inspected HST WFPC2 F547M and F656N imaging (GO 7273) of Circinus (Wilson et al. 2000). No cluster is detected at the location of SN 1996cr, although compact Hα emission is confirmed, potentially resulting from the SN itself, in part.

A17 SN 1997X in NGC 4691

SN 1997X was discovered in Feb 1997, approximately 9″ E of the centre of NGC 4691 (Nakano et al. 1997). Using the inclination and major axis PA from HyperLeda this corresponds to a deprojected offset of 11″ (0.14 R_{25}) or 0.7 kpc for a 12 Mpc distance to NGC 4691. Although we do not have access to calibrated Hα imaging of NGC 4691, Anderson & James (2008) discuss INT/WFC imaging, from which a normalized cumulative rank (NCR) pixel value of 0.323 is obtained for SN 1997X. Munari et al. (1998) report nebular Hα+[N II] emission from a H II region superimposed upon an early spectrum of this type Ib supernova (Modjaz et al., in prep.). Figure A15 presents the INT Hα imaging from Mar 2007, from which we note diffuse nebular emission centred upon the nucleus of NGC 4691, extending ±15″ east-west, Superimposed upon the diffuse nebular emission are several spatially extended knots, the brightest of which lies 6″ (0.4 kpc) WSW of the SN location.

A18 SN 1998dn in NGC 337A

SN 1998dn was discovered in Aug 1998 in NGC 337A, 2.1′ SW of its nucleus (Cao 1998), corresponding to a deprojected offset of 3.5′ (1.2 R_{25}) or 11.6 kpc based on a 11.4 Mpc distance to NGC 337A. JHK Hα imaging from Apr 2002 (Knapen et al. 2004) is presented in Fig. A16 and shows that this type II SN lies in a region devoid of nebular emission, with the nearest bright H II region 5″.5 to the NW, which corresponds to a deprojected distance of 0.5 kpc for the HyperLeda inclination and PA.

A19 SN 1999em in NGC 1637

This type II-P supernova was discovered in Oct 1999, 24″ SW of the nucleus of NGC 1637 (Li 1999; Jha et al. 1999), corresponding to a deprojected offset of 27″ (0.22 R_{25}) which is equivalent to a galactocentric distance of 1.3 kpc for a 9.77 Mpc distance to NGC 1637. As shown in Fig. A17, SN 1999em was still very bright in Oct 2000 when the CTIO 1.5m Hα imaging of Meurer et al. (2006) was obtained. We have therefore inspected pre-SN Hα imaging from Ryder & Dopita (1993) obtained with the Siding Spring 40″

telescope which indicates negligible nebular emission at the SN site. The closest H II region to the SN location lies 6″ (0.3 kpc) SE and has a luminosity comparable to the Orion nebula. Other H II regions to the NW and SW each lie 7″ (375 pc) away, with Hα+[N II] fluxes of 1.7×10^{-15} erg s^{-1} cm^{-2} and 3.1×10^{-15} erg s^{-1} cm^{-2}, respectively. A brighter source lies 9″.5 (0.5 kpc) to the SE, with a luminosity comparable to the Rosette nebula. Smartt et al. (2002) analysed Jan 1992 broad-band imaging from 3.6m CFHT in which the progenitor was undetected, i.e. there is no evidence for an host cluster. Note that the SN is detected in HST WFPC2 F555W imaging (GO 9155, PI D.C. Leonard) obtained in Sep 2001.

A20 SN 1999eu in NGC 1097

This type II-P supernova was discovered in Nov 1999 (Nakano et al. 1999a) within a spiral arm of NGC 1097, 2.6′ to the SSE of its nucleus. This corresponding to a de-projected galactocentric distance of 3.9′ (0.83 R_{25}) or 16 kpc for the HyperLeda inclination and major axis PA plus an EDD distance of 14.2 Mpc. Fig. A18 presents CTIO 1.5m Hα imaging from Oct 2001 (Kennicutt et al. 2003), revealing no nebular emission at the position of SN 1999eu. The closest H II region lies 3″.75 ± to the W, at a deprojected distance of 375 pc, and is spatially extended EW, while a brighter complex with a Hα+[N II] flux of $2.5{\times}10^{-15}$ erg s^{-1} cm^{-2} (3 arcsec aperture radius) lies 13″ (1.3 kpc deprojected) to the E.

A21 SN 1999gi in NGC 3184

SN 1999gi was discovered in Dec 1999, 1′ north of the nucleus of NGC 3184 (Nakano et al. 1999b), whose low inclination of 14° implies negligible projection effects (0.28 R_{25}), such that the galactocentric distance is 3.9 kpc based on a 13 Mpc distance to NGC 3184. Fig. A19 shows KPNO 2.1m Hα imaging from Apr 2002 (Kennicutt et al. 2003) which reveals diffuse emission at the position of the SN, intermediate between extended H II regions 2″ (125 pc) to the SW and NE. The former has a Hα luminosity comparable to the Rosette nebula, while the latter is more extended and has a luminosity a factor of ∼3 times higher. Within the larger star forming complex, additional knots lie 6″.9 (430 pc) to the SW and 10″ (630 pc) to the NE, with Hα+[N II] fluxes of $4{\times}10^{-15}$ erg s^{-1} cm^{-2} and $1{\times}10^{-14}$ erg s^{-1} cm^{-2}, respectively. Pre-SN WFPC2/WF images obtained wth the F606W filter in Jun 1994 (GO 5446, PI G.D. Illingworth), identify nearby OB stars but not the progenitor of the type II-P supernova, while the SN is detected in WFPC2/PC F555W images (GO 8602, PI A.V. Filippenko) from Jan 2001 (Smartt et al. 2001; Leonard et al. 2002; Hendry 2006).

A22 SN 2001X in NGC 5921

This type II-P supernova was discovered in Feb 2001, 33″ SSW of the nucleus of NGC 5921 (Li et al. 2001). For the HyperLeda inclination and major axis PA, this deprojects to 49″ (0.34 R_{25}) or 3.4 kpc, with a scale of 1″ = 100 pc for the 14 Mpc distance to NGC 5921. From inspection of the net Hα imaging from Apr 2001 (James et al. 2004), SN 2001X was exceptionally bright. Fig. A20 shows the JKT Hα imaging from Mar 1999, plus R-band imaging from Mar 2003 to assess the nebular environment. SN 2001X is coincident with faint nebulosity, while extended emission lies 3″ (0.3 kpc) SE of SN 2001X, comparable in luminosity to the Rosette nebula. A brighter compact source lies 4″ to the N (0.4 kpc), although SN 2001X is not strictly associated with either. Anderson et al. (2012) quote a NCR pixel value of 0.698 for SN 2001X based on Liverpool Telescope imaging from Apr 2009, obtained archival indicating a potential contribution from the SN remnant.

A23 SN 2001ig in NGC 7424

SN 2001ig (IIb) was discovered by R. Evans in Dec 2001, 2.95′ NE of the nucleus of NGC 7424 (Evans et al. 2002). Based on the HyperLeda inclination of NGC 7424 and an adopted PA of the major axis of 0, the deprojected distance is 4′.9 (1.0 R_{25}) or 11.2 kpc for the adopted distance of 7.94 Mpc. Fig. A21 presents pre-explosion CTIO 1.5m Hα imaging from Sep 2000 (Meurer et al. 2006). The figure shows that SN 2001ig occurred at the periphery of a modest luminosity (Orion-like), extended H II region. Faint diffuse emission is also detected 6–10″ to the S of the supernova, at a deprojected distance of 0.4–0.6 kpc. A brighter H II region, with F(Hα+[N II]) = $2.5{\times}10^{-15}$ erg s^{-1} cm^{-2} (2″.5 radius aperture), is located 17″ to the SW, corresponding to a deprojected distance of 1.1 kpc. Astrometry was verified from VLT/FORS2 R-band imaging of SN 2001ig obtained in Jun 2002 (069.D-0453, PI E.Cappellaro). High spatial resolution u', g', r' Gemini GMOS imaging from Sep 2004 is discussed by Ryder et al. (2006), who remark upon arcs of diffuse nebulosity from their deep u' imaging.

A24 SN 2002ap in M 74

This well studied type Ic supernova was discovered by Y. Hirose in Jan 2002 in the outer disk of M 74, 4.7′ (0.89 R_{25}) SW of the nucleus (Nakano et al. 2002). The low inclination of M 74 (Kamphuis & Briggs 1992) implies that deprojection effects are negligible, such that the galactocentric distance is 12.2 kpc for a 9 Mpc distance to M 74. Its location was beyond the field-of-view of VLT/FORS1 and VATT 1.8m imaging, so we present CTIO 1.5m Hα imaging from Oct 2001 (Kennicutt et al. 2003) in Fig. A22. The closest nebular emission to SN 2002ap is an extended, Orion-like, H II region 10″ (0.4 kpc) to the SSE. Additional sources lie 17″ (0.75 kpc) and 22″ (1 kpc) to the SE, the latter with a Hα+[N II] flux of $4{\times}10^{-15}$ erg s^{-1} cm^{-2} (4″ radius aperture).

Crockett et al. (2007) present deep, 3.6m CFHT broad-band imaging from Oct 1999, together with post-SN HST ACS/HRC imaging from Jan 2003–Aug 2004 from which the progenitor star could not be identified. We have also inspected CFHT/CFH12K Hα images of the site of SN2002ap from Jun 1999 (PI J.-C. Cuillandre) which confirm the CTIO results, while nebular emission is not detected in shallow HST ACS/HRC F658N images from Jan 2003 (GO 9144, PI R.P. Kirschner).

A25 SN 2002hh in NGC 6946

This type II-P supernova was discovered in Oct 2002, 2.2′ (0.4 R_{25}) SW of the nucleus of NGC 6946 (Li 2002), corresponding to 4.5 kpc for the adopted distance of 7 Mpc to NGC 6946 (3″ approximates to 100 pc). Fig. A23 presents our Oct 2009 Gemini GMOS Hα imaging. SN 2002hh occurred close to the periphery of an extended giant H II region 1″.5–3″.5 (50–120 pc) to its NW, whose radius is ∼ 4″. In addition, a faint knot of nebular emission is observed at the position of SN 2002hh, likely arising from the SNR, with a Hα+[N II] flux of $4{\times}10^{-16}$ erg s^{-1} cm^{-2} (1″ radius aperture), corresponding to a luminosity several times lower than Orion. As discussed by e.g. Otsuka et al. (2012), SN 2002hh is detected in F606W filter observations with HST ACS/HRC from Sep 2005

(GO 10607, PI. B.Sugerman) and WFPC2/PC images from July 2007 (GO 11229, PI M. Meixner). In addition, the extended nebular emission to the NW is spatially resolved in ACS/HRC F658N imaging from Sep 2005, with the brightest knot 2″.3 (80 pc) NW of SN 2002hh.

A26 SN 2003B in NGC 1097

SN 2003B (II-P) was discovered by R. Evans in Jan 2003, 3′ NW of the nucleus of NGC 1097 (Evans & Quirk 2003), equivalent to a galactocentric distance of 4.9′ (1.04 R_{25}) or 20 kpc for the 14.2 Mpc distance to NGC 1097. Fig. A24 presents CTIO 1.5m Hα imaging from Oct 2001 (Kennicutt et al. 2003). SN 2003B lies at the periphery of a spatially extended H II region, cited in early spectroscopy of SN 2003B by Kirshner & Silverman (2003). The luminosity of this giant H II region is comparable to N66 in the SMC.

A27 SN 2003gd in M 74

This type II-P supernova was also discovered by R. Evans in Jun 2003, 2.7′ (0.51 R_{25}) SSE of the nucleus of M 74 (Evans & McNaught 2003). As for SN 2002ap, deprojection effects are negligible owing to the low inclination of M 74 (Kamphuis & Briggs 1992), so the galactocentric distance is 7.0 kpc based on our 9 Mpc distance. The location of the SN is intermediate between three large, star forming complexes to the SW, NE and NW (Hodge 1976). Fig. A25 presents the Oct 2007 VLT/FORS1 imaging, for which the precise SN location is identified from differential astrometry using post-explosion HST ACS/HRC F555W observations from Aug 2003 (GO 9733, PI S.J. Smartt). Diffuse nebulosity is observed several arcsec to the NE of SN 2003gd, whose integrated Hα+[N II] flux of $4{\times}10^{-16}$ erg s^{-1} cm^{-2} (1″.5 radius aperture) implies a luminosity significantly inferior to the Orion nebula.

The closest H II regions to SN 2003gd are compact sources to the N and SW, each 7″ (0.3 kpc) away, catalogued as #641 and #640 from Hodge (1976), respectively. Each has a luminosity comparable to the Orion nebula. The main complex of the SW nebulosity (#639 from Hodge 1976) peaks 12″ (0.5 kpc) from SN 2003gd, and has a Hα+[N II] flux an order of magnitude larger. The luminosity of another complex, #636 and #637 from Hodge (1976), which peaks 18″ (0.8 kpc) to the NW of the SN, is comparable to N66 in the SMC, while the complex 15″ to the NE (#649–651 from Hodge 1976) has an intermediate luminosity. Hendry et al. (2005) refer to the NW complex in their study of SN 2003gd via #72–73 from Belley & Roy (1992).

HST ACS/HRC F625W imaging (GO 10272, P.I. A.V. Filippenko) also reveals very faint nebulosity several arcsec W of the SN position, while no cluster is seen at the site of the SN. Pre-SN HST WFPC2 and Gemini GMOS imaging from May-Aug 2002 enabled Smartt et al. (2004) to identify a red supergiant as the progenitor of SN 2003gd (see also Maund & Smartt 2009).

A28 SN 2003jg in NGC 2997

This type Ib/c supernova was discovered by R. Martin in Oct 2003, 13″ NW of the nucleus of NGC 2997 (Martin & Biggs 2003), which deprojects to 18″ (0.07 R_{25}) or a galactocentric distance of 1.0 kpc using a 11.7 Mpc distance to NGC 2997. This galaxy is undergoing an intense, ring-like star formation episode in its nucleus, with a luminosity comparable to 30 Doradus in the LMC. Fig. A26 presents Danish 1.5m Hα images (Larsen & Richtler 1999), revealing that SN 2003jg lies 2″ (140 pc) W of a modest, Orion-like H II region, apparently associated with this intense activity. It is unclear whether this region is extended from the Danish 1.5m imaging, so we have examined high quality VLT/FORS1 R-band imaging from Mar 1999 (60.A-9203), which indicate that the source is spatially extended NS. No source is coincident with the SN progenitor based on HST WFPC2 imaging from Aug 2001 using the F450W filter (GO 9042, PI S.J. Smartt).

A29 SN 2004dj in NGC 2403

SN 2004dj (II-P) was discovered by K. Itagaki in July 2004, 2.7′ east of the nucleus of NGC 2403 (Nakano et al. 2004). Based on the inclination and PA of the major axis of NGC 2403 from HyperLeda, this corresponds to a deprojected distance of 3.7′ (0.34 R_{25}) or 3.4 kpc for a 3.16 Mpc distance to NGC 2403, the second closest ccSNe in our sample. Figure. A27 shows KPNO 2.1m Hα observations of NGC 2403 from Nov 2001 (Kennicutt et al. 2003), while we have also inspected higher spatial resolution Hα observations of the central region of NGC 2403 from NOT/ALFOSC (Larsen & Richtler 1999).

Maíz-Apellániz et al. (2004) identified SN 2004dj with a young, compact star cluster, #96 from Sandage (1984). From Fig. A27, this is not a source of Hα emission, with the faint, diffuse emission ∼8″ to the SE, a deprojected distance of 170 pc away. The nearest prominent star forming regions each lie 21″ (450 pc) NW and SE. The former H II region is spatially extended, albeit relatively compact, with a luminosity similar to the Rosette nebula, while the latter contains multiple knots, separated by several arcsec and has an integrated luminosity comparable to N66.

Vinkó et al. (2006, 2009) have studied Sandage 96, from which both 'young' (10–16 Myr, 15–20 $M_{\odot}$) and 'old' (30–100 Myr, < 10$M_{\odot}$) solutions were obtained. From post-explosion 2.3m Bok Hα imaging, they also note that Sandage 96 lacks extended Hα emission and attribute the bulk of the compact Hα emission that they detected to SN 2004dj itself. Diffuse emission is not detected in HST ACS/HRC F658N imaging from Aug 2005 (GO 10607, PI B.E. Sugerman), while the compact nature of the NW source is confirmed from HST WFPC2 F606W imaging from Apr 2008 (GO 11229, PI M. Meixner).

A30 SN 2004et in NGC 6946

This type II-P supernova was discovered by S. Moretti in Sep 2004, 4.5′ (0.8 R_{25}) SE of the nucleus of NGC 6946 (Zwitter et al. 2004) corresponding to a galactocentric distance of 9.6 kpc based on a 7.0 Mpc distance to NGC 6946. This region, far from any large star forming regions, falls beyond the field-of-view of the Gemini GMOS imaging, so Fig. A28 shows KPNO 2.1m Hα imaging from Mar 2001 (Kennicutt et al. 2003). The closest nebular emission lies 9″ (300 pc) N of the position of SN 2004et, extends NE–SW over several arcsec, and has an integrated luminosity comparable to the Orion nebula. Crockett et al. (2010) discuss constraints upon the progenitor of SN 2004et from various facilities, including pre-SN CFHT/CFH12K R-band imaging and post-SN HST WFPC2/PC (GO 11229, P.I. M. Meixner) F606W imaging from Jan 2008, with a second (point) source detected 0″.25 E of the SN position. The extended nebular emission N of SN 2004et is apparent in both datasets.

A31 SN 2005at in NGC 6744

This type Ic supernova was jointly discovered by R. Martin and L. Monard in Mar 2005, 2′.3 NNE of the nucleus of NGC 6744 (Martin et al. 2005), corresponding to a galactocentric distance of 3′.0 (0.30 R_{25}) or 10.0 kpc for a 11.6 Mpc distance to NGC 6744. In Fig. A29 we present our VLT/FORS1 continuum-subtracted Hα imaging from Jun 2008. The SN occurred within an extended H II region whose luminosity is comparable to the Rosette nebula. This nebula is also detected in pre-SN Danish 1.5m imaging from Feb 1998 (Larsen & Richtler 1999). The faint continuum source at the position of SN 2005at in Fig. A29 is likely due to the SNR itself. A bright continuum source lies 8″.5 S of SN 2005at, at a deprojected distance of 0.6 kpc, which is poorly subtracted in the VLT/FORS1 net Hα image. The SN has also been imaged with HST WFPC2/PC using the F555W filter (GO 10877, PI W. Li) in Apr 2007.

A32 SN 2005cs in M 51a

This type II-P supernova was discovered by W. Kloehr in June 2005, within a complex star forming region, 1.1′ (0.2 R_{25}) SSW of the nucleus of M 51a (Kloehr et al. 2005), with negligible projection effects, such that the galactocentric distance is 2.7 kpc for a 8.39 Mpc distance to M 51a. Fig. A30 presents KPNO 2.1m imaging from Mar 2001 (Kennicutt et al. 2003), revealing that SN 2005cs coincides with a region of nebular emission extending N-S. Orion-like H II regions are located 1″ (40 pc) E, 2″.7 (110 pc) N and 4″.3 (175 pc) E, while brighter star forming knots are located >9″ (>0.35 kpc) to the N, NE and E, the brightest of which is spatially extended N-S, lies 13″ (0.55 kpc) E of the SN and has a luminosity comparable to the Rosette nebula. These sources are poorly resolved in ground-based R-band imaging, except that by far the brightest continuum source is that 9″ NE of the SN.

We have inspected HST ACS/WFC (GO 10452, PI S. Beckwith) images obtained with the F555W and F658N (Hα+[N II]) filters in Jan 2005. As shown in Fig. 2, SN 2005cs is not associated with nebular emission, although compact Hα sources lie 1″ (40 pc) to the SE and NE, plus there is a compact star cluster ∼0″.2 (8 pc) to the SW (see Li et al. 2006).

A33 SN 2005kl in NGC 4369

SN 2005kl was discovered by M. Migliardi in Nov 2005, 10″ (0.17 R_{25}) NW of the centre of NGC 4369 (Migliardi et al. 2005). In view of the low inclination of this galaxy (18.9°), there are negligible projection effects, so the galactocentric distance is 0.6 kpc for a 11.2 Mpc distance to NGC4369. Although we do not have access to calibrated Hα imaging of NGC 4369, Fig. A31 presents Liverpool Telescope RATCam Hα and (Sloan) r′-band imaging of NGC 4369 from Feb 2007 (Anderson & James 2008). This type Ic supernova occurred at the periphery of a bright, spatially extended H II region, the peak of which lies 1″.5 (80 pc) to the SE of the supernova, with the main (continuum) body of the galaxy further to the E. Anderson & James (2008) quote a normalized cumulative rank (NCR) pixel value of 0.570 from their RATCam imaging.

A34 SN 2007gr in NGC 1058

This type Ic supernova was discovered by W. Li in Aug 2007, 0.5′ NW of the nucleus of NGC 1058 (Li et al. 2007), corresponding to a deprojected offset of 0.7′ (0.45 R_{25}) for the HyperLeda inclination and major axis PA, i.e. a 2.0 kpc galactocentric distance for the 9.86 Mpc distance to NGC 1058. This SN occurred within a large star forming complex (Crockett et al. 2008). Fig. A32 shows 2.3m Bok imaging obtained in Nov 2003 (Kennicutt et al. 2008), in which the primary source of Hα emission within this complex is a giant H II region, comparable in luminosity to the SMC's N66. This lies ∼2″ W of SN 2007gr, corresponding to a deprojected distance of 130 pc, and itself is spatially extended. Diffuse nebular emission is found at the location SN 2007gr, while another bright component is observed 1″.5 to the NW, with a luminosity similar to the Rosette nebula. Anderson et al. (2012) quote a NCR pixel value of 0.157 for SN 2007gr based on JKT imaging. Crockett et al. (2008) have studied pre- and post-SN images of NGC 1058 including archival INT imaging. INT/WFC Hα and r'-band imaging from Jan 2005 reveal bright, spatially extended emission 2″.7 (170 pc) W of the SN location, plus faint nebulosity 1″ to the S, and to the E. More recent HST WFPC2/F675W imaging from Nov 2008 (GO 10877, PI W. Li) and WFC3/F625W imaging from Jan 2010 (GO 11675, PI J. Maund) indicate fainter nebulosity at the SN position.

A35 SN 2008bk in NGC 7793

This type II-P supernova was discovered in Mar 2008, offset 2.1′ NNE of the nucleus of NGC 7793 (Monard 2008a). This corresponds to a deprojected radial offset of 3.5′ (0.75 R_{25}) for the adopted inclination and PA (Carignan & Puche 1990), equivalent to 3.7 kpc for a 3.61 Mpc distance to NGC 7793. Since this position lays beyond the field-of-view of our VLT/FORS1 Hα images, so Fig. A33 presents continuum subtracted CTIO 1.5m Hα images from Oct 2001 (Kennicutt et al. 2003). SN 2008bk is neither spatially coincident with nebular emission nor a bright continuum source. A Hα arc extends to the N and W of the SN position, ∼6″ away, corresponding to a deprojected distance of 175 pc, and connects to a spatially extended H II region, 7″ (200 pc) to the SW. In addition to this source, which is somewhat more luminous than the Orion nebula, other fainter star formation knots lie 11–12″ to the S and SE of SN 2008bk. Mattila et al. (2008) and van Dyk et al. (2012) confirm a red supergiant progenitor for SN 2008bk from, respectively, pre-explosion VLT/FORS1 and Gemini/GMOS imaging. Archival VLT/FORS1 Hα and R-band imaging from Sep 2001 (067.D-0006(A)), the former uncalibrated, confirm the nebular morphology of CTIO 1.5m imaging. Post-SN F814W imaging has also been obtained with HST WFC3 from Apr 2011 (GO 12262, PI J.R. Maund).

A36 SN 2008eh in NGC 2997

This probable type Ib/c supernova (Horiuchi et al. 2011) was discovered in July 2008, 2.1′ ENE of the nucleus of NGC 2997 (Monard 2008b), close to its major axis, such that the deprojected radial distance is 2′.2 (0.5 R_{25}) or 7.4 kpc for a 11.3 Mpc distance to NGC 2997. Fig. A34 shows the site of SN 2008eh at the periphery of a giant H II region, 2″ (110 pc) to the SW, based on 1.5m Danish Hα imaging of Larsen & Richtler (1999). A brighter, N66-like, giant H II region 4″.5 (250 pc) lies to the S. Both sources are prominent in R-band images.

A37 SN 2009N in NGC 4487

This type II-P supernova was discovered by K. Itagaki in Jan 2009, 1.3′ ENE of the nucleus of NGC 4487 (Nakano et al. 2009), which corresponds to a deprojected radial distance of 1.6′ (0.77 R_{25}) or

5.1 kpc for a 11 Mpc distance to NGC 4487. Figure A35 shows continuum-subtracted JKT Hα imaging (Knapen et al. 2004), from which we identify a compact H II region 3″ to the NW, a deproject distance of 200 pc away, with a luminosity comparable to the Orion nebula. In addition, a more extended H II region lies 3″ (200 pc) to the NE, closer in luminosity to the Rosette nebula. SN 2009N is not associated with either of these star forming regions.

A38 SN 2009ib in NGC 1559

SN 2009bi (II-P) was disovered in Aug 2009, 37″ NE of the centre of NGC 1559 (Pignata et al. 2009). This corresponds to a radial distance of 70″ (0.67 R_{25}) or galactocentric distance of 4.2 kpc for a 12.6 Mpc distance to NGC 1559. Fig. A36 shows pre-SN VLT/FORS1 continuum subtracted Hα imaging from Aug 2005. Faint nebulosity is observed at the site of the SN, with an extended H II region 1″.5 to the SE, a deprojected distance of 170 pc away. Extended, giant H II regions lie to the W of SN 2009bi, including a source 6″ (0.7 kpc) SW of the SN comparable in luminosity to N66, plus a supergiant H II region 13″ (1.5 kpc) to the ESE with a Hα+[N II] flux of 1.5×10^{-13} erg s^{-1} cm^{-2} (2″.5 aperture radius). Pre-SN HST imaging with WFPC2 using the F606W filter (GO 9042, PI S.J. Smartt) reveals a potential host cluster within the error circle of the SN location, plus diffuse nebular emission.

A39 SN 2011dh in M 51a

This type IIb supernova was discovered in late May 2011, 2.6′ SE of the nucleus of M 51a (Griga et al. 2011), corresponding to a radial distance of 2′.8 (0.5 R_{25}) or 6.8 kpc for a 8.39 Mpc distance to M 51a. Fig. A37 shows that the SN position is close to the centre of a ring of star forming regions, based on KNPO 2.1m Hα imaging (Kennicutt et al. 2003). Of these, the closest to the site of the SN lies 8″ (0.35 kpc) SE and has a similar luminosity to the Rosette nebula. Other, spatially extended, giant H II region complexes lie 11–13″ to the NE, NW and SW. Anderson et al. (2012) report a NCR pixel value of 0.00 for SN 2011dh from INT imaging, while inspection of archival HST ACS/WFC images confirms the absence of nebular emission at the position of SN 2011dh. The (point source) SN progenitor is detected in ACS/WFC F555W and F658N images (e.g. van Dyk et al. 2011; Maund et al. 2011), which also resolve the star forming region to the SE into two main components, separated by 1″.0 (45 pc). H II regions to the NE and NE are largely dominated by one main component, while that to the SW is highly complex, comprising multiple compact sources.

A40 SN 2012A in NGC 3239

This type II-P supernova was discovered in Jan 2012, is 50″ SE of the nucleus of NGC 3239 (Moore et al. 2012). Based on the HyperLeda inclination of NGC 3239, this corresponds to a radial distance of 64″ (0.42 R_{25}) for this galaxy, corresponding to 3.1 kpc at 10 Mpc. Fig. A38 presents continuum-subtracted Hα and R-band imaging from VATT 1.8m (Kennicutt et al. 2008). SN 2012A is located close to a very bright star forming complex, although it is neither spatially coincident with nebular emission nor a continuum source. An extended nebula with a luminosity comparable to the Rosette nebula lies 2″ (120 pc) to the S, with the main complex extending over several hundred pc due E of the SN. Within this region, the closest knot of star formation lies 7″ (0.4 kpc) to the E of the SN and has an integrated Hα+[N II] flux of 2×10^{-14} erg s^{-1} cm^{-2} (2″ aperture radius), comparable to N66 in the SMC. Supergiant H II regions are found 10″ (0.6 kpc) to the NE and 12″ (0.75 kpc) to the SE, each similar to NGC 604 in luminosity.

A41 SN 2012aw in M 95

This type II-P supernova was discovered in Mar 2012, 2′.1 SW of the nucleus of M 95 (NGC 3351). This corresponds to a radial distance of 2′.3 (0.62 R_{25}) using an inclination and PA of its major axis from HyperLeda, i.e. a galactocentric distance of 6.7 kpc at 10 Mpc. Continuum-subtracted Hα imaging from KPNO 2.1m (Kennicutt et al. 2003) is presented in Fig. A39. Nebular emission is not observed at the site of the SN, with a H II region 5″ (260 pc) to the NNE, somewhat less luminous than the Orion nebula. A further pair of faint H II regions are located 7″ (370 pc) to the W, plus an extended H II region 10″ (525 pc) to the SW that is comparable to the Orion nebula. The closest giant H II regions lie 19″ (1.0 kpc) SSE and 22″ (1.2 kpc) ENE, with the integrated Hα+[N II] flux of the former 4×10^{-14} erg s^{-1} cm^{-2} (4″ aperture radius), implying a luminosity comparable to N66 (SMC). HST WFPC2 imaging of the site of SN 2012aw was obtained in Nov 1994 using the F555W filter (GO 5397, PI J. Mould).

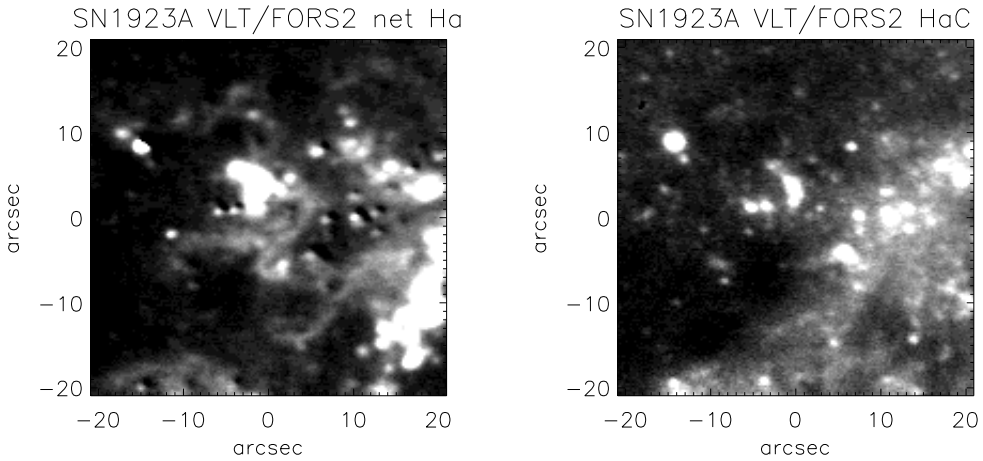

Figure A1. (left) VLT/FORS2 net Hα image (from Hadfield et al. 2005) showing the nebular environment of SN 1923A (at centre of image, Class 5). The 42×42 arcsec^2 field of view projects to 1×1 kpc^2 at the 4.9 Mpc distance of M 83; (right) Continuum image (λ_c = 6665Å). North is up and east is to the left for these and all subsequent images.

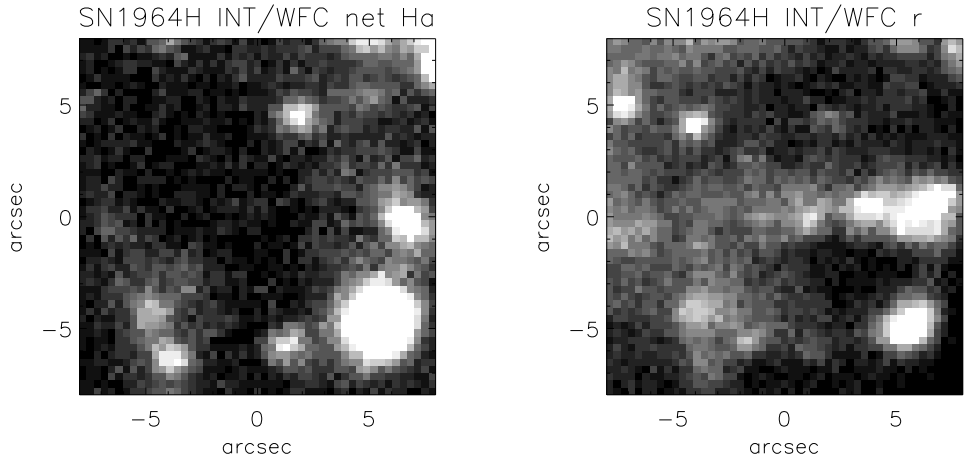

Figure A2. (left) INT/WFC net Hα image showing the nebular environment of SN 1964H (at centre of image, Class 2). The 16×16 arcsec^2 field of view projects to 1×1 kpc^2 at the 12.9 Mpc distance of NGC 7292; (right) r-band image.

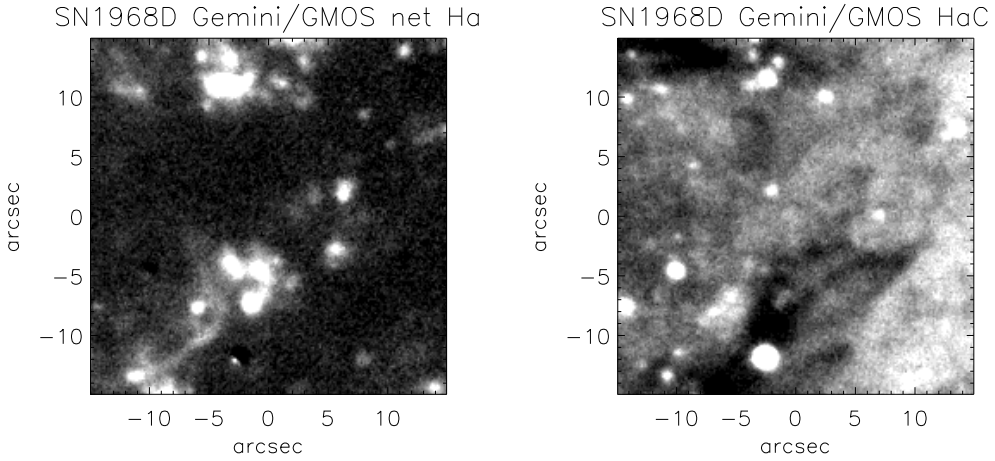

Figure A3. (left) Gemini/GMOS net Hα image (from GN-2009B-Q-4) showing the nebular environment of SN 1968D (at centre of image, Class 2). The 30×30 arcsec^2 field of view projects to 1×1 kpc^2 at the 7.0 Mpc distance of NGC 6946; (right) Continuum image (λ_c = 6620Å).

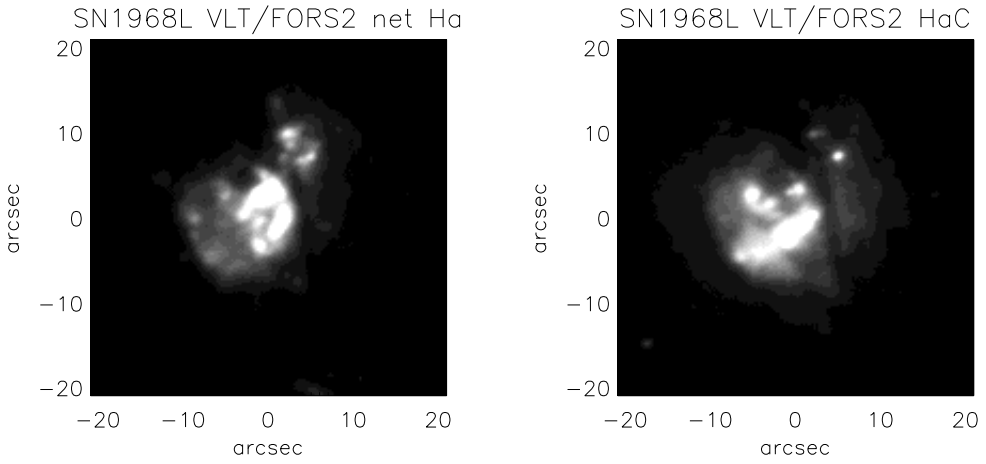

Figure A4. (left) VLT/FORS2 net Hα image (from Hadfield et al. 2005) showing the nebular environment of SN 1968L (at centre of image, Class 5). 42×42 arcsec^2 field of view projects to 1×1 kpc^2 at the 4.9 Mpc distance of M 83; (right) Continuum image (λ_c = 6665Å).

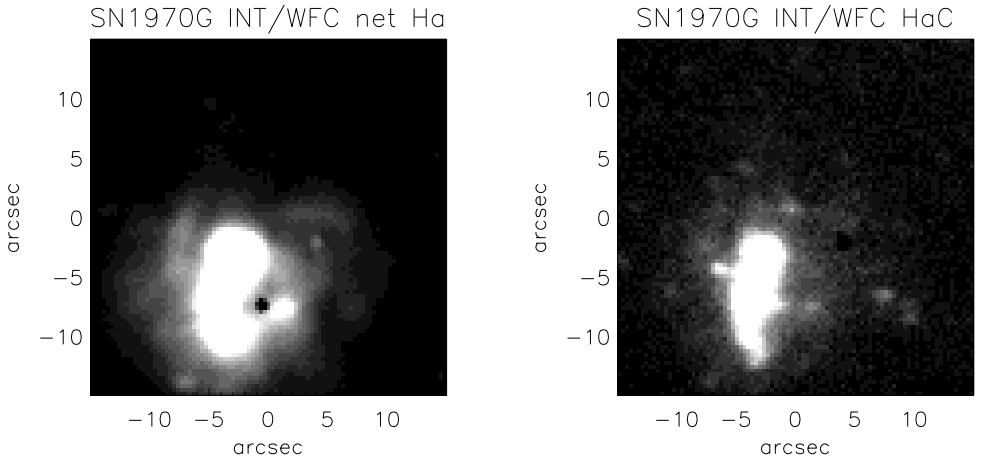

Figure A5. (left) INT/WFC net Hα image showing the nebular environment of SN 1970G (at centre of image, Class 5). The 30×30 arcsec^2 field of view projects to 1×1 kpc^2 at the 6.96 Mpc distance of M 101; (right) Continuum image (λ_c = 6657Å).

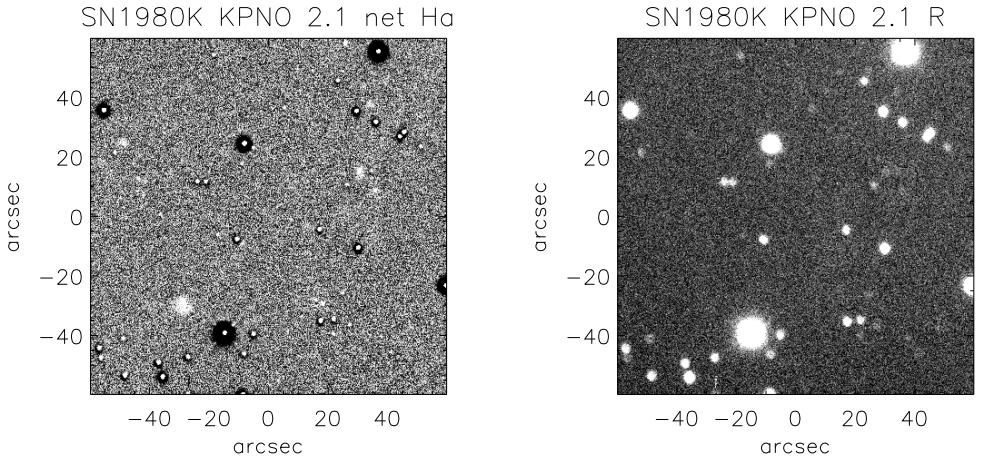

Figure A6. (left) KPNO 2.1m net Hα image (from Kennicutt et al. 2003) showing the nebular environment of SN 1980K (at centre of image, Class 2). Bright field stars are poorly subtracted. The 120×120 arcsec^2 field of view projects to **4×4** kpc^2 at the 7 Mpc distance of NGC 6946; (right) R-band image.

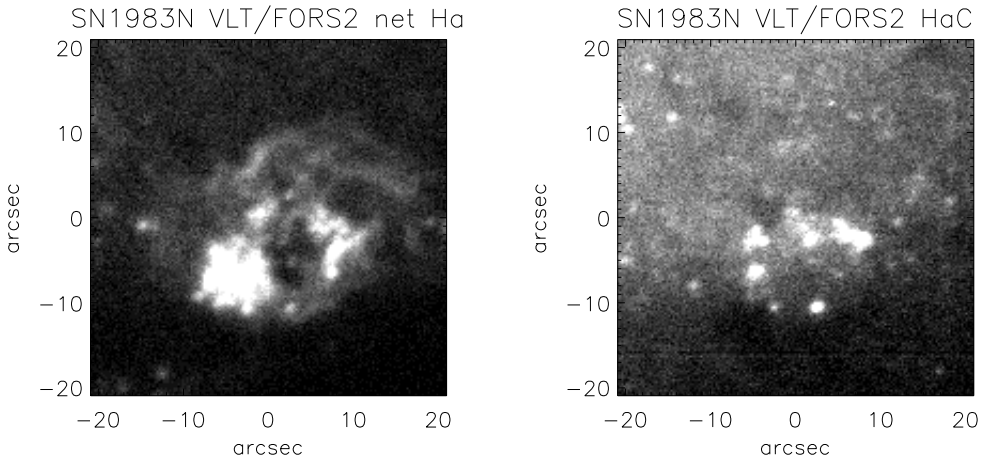

Figure A7. (left) VLT/FORS2 net Hα image (from Hadfield et al. 2005) showing the nebular environment of SN 1983N (at centre of image, Class 4). The 42×42 arcsec^2 field of view projects to 1×1 kpc^2 at the 4.9 Mpc distance of M 83; (right) Continuum image (λ_c = 6665Å).

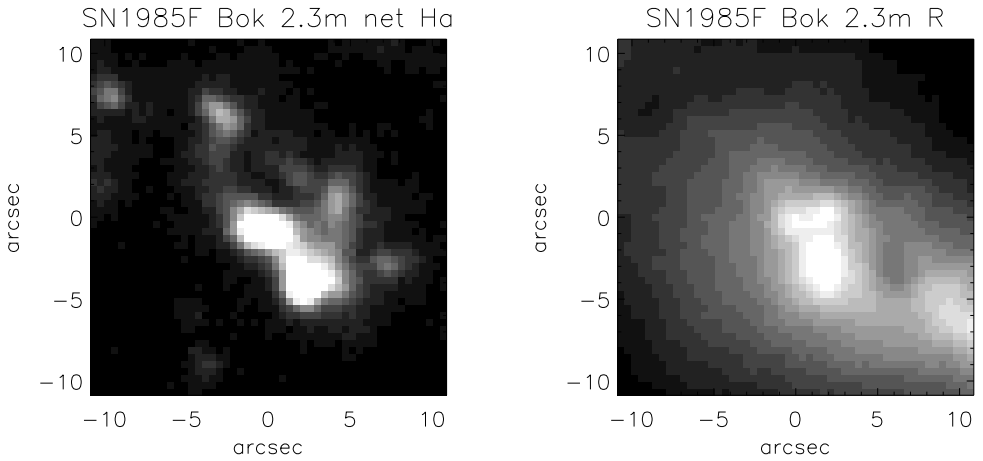

Figure A8. (left) Bok 2.3m net Hα image (from Kennicutt et al. 2008) showing the nebular environment of SN 1985F (at centre of image, Class 5). The 22×22 arcsec^2 field of view projects to 1×1 kpc^2 at the 9.2 Mpc distance of NGC 4618; (right) R-band image.

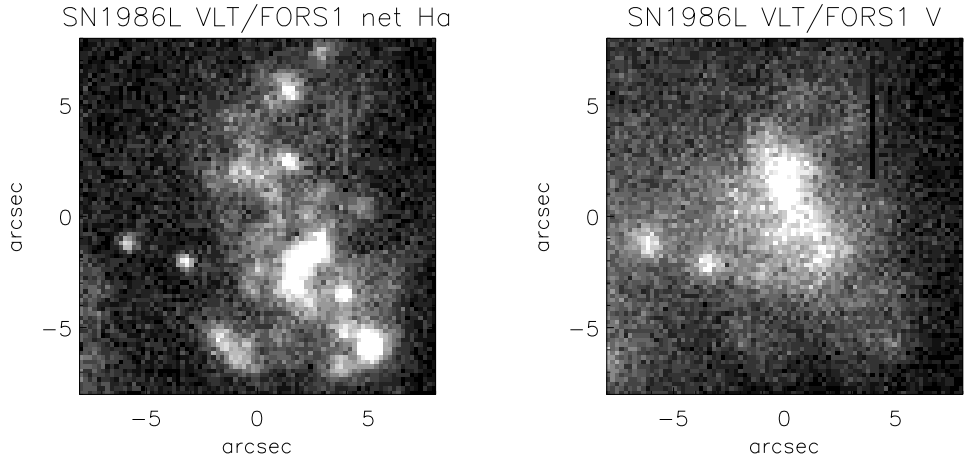

Figure A9. (left) VLT/FORS1 net Hα image (from 075.D-0213(A)) showing the nebular environment of SN 1986L (at centre of image, Class 3). The 16×16 arcsec^2 field of view projects to 1×1 kpc^2 at the 12.6 Mpc distance of NGC 1559; (right) V-band image.

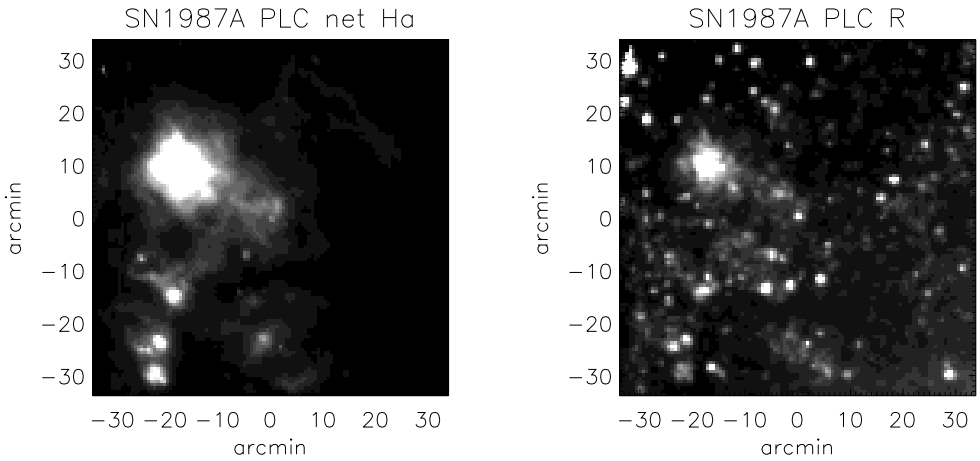

Figure A10. (left) Parking Lot Camera net Hα image (from Kennicutt et al. 1995) showing the nebular environment of SN 1987A (at centre of image, Class 4). The 68×68 arcmin^2 field of view projects to 1×1 kpc^2 at the 50 kpc distance of the LMC; (right) R-band image (from Bothun & Thompson 1988).

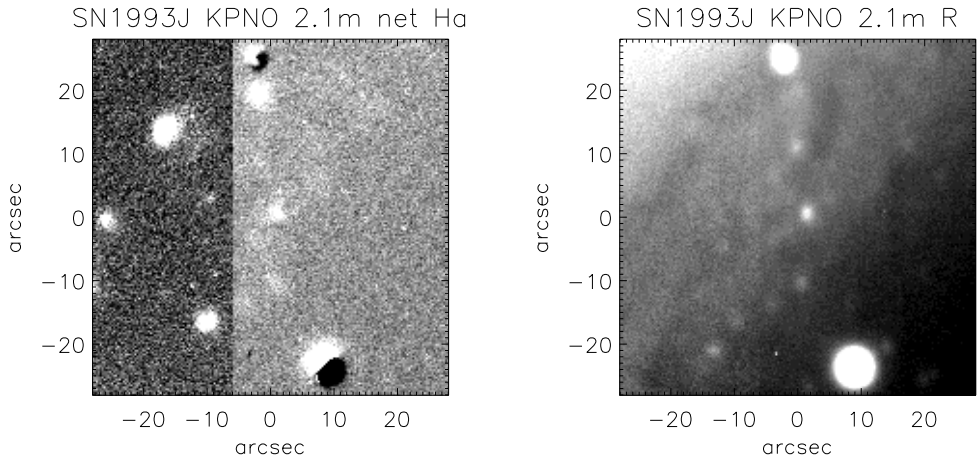

Figure A11. (left) KPNO 2.1m net Hα image (from Kennicutt et al. 2003) showing nebular emission close to the position of SN 1993J (at centre of image, Class 2). The 56×56 arcsec^2 field of view projects to 1×1 kpc^2 at the 3.6 Mpc distance of M 81. The apparent change in sky background arises from the mosaicing of several pointings of M 81; (right) R-band image.

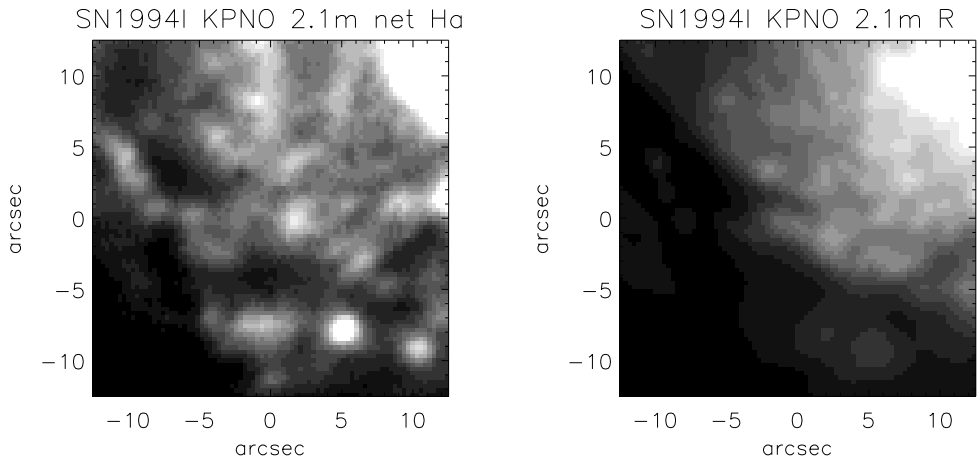

Figure A12. (left) KPNO 2.1m net Hα image (from Kennicutt et al. 2003) showing nebular emission close to the position of SN 1994I (at centre of image, Class 5). The 25×25 arcsec^2 field of view projects to 1×1 kpc^2 at the 8.4 Mpc distance of M 51a; (right) R-band image.

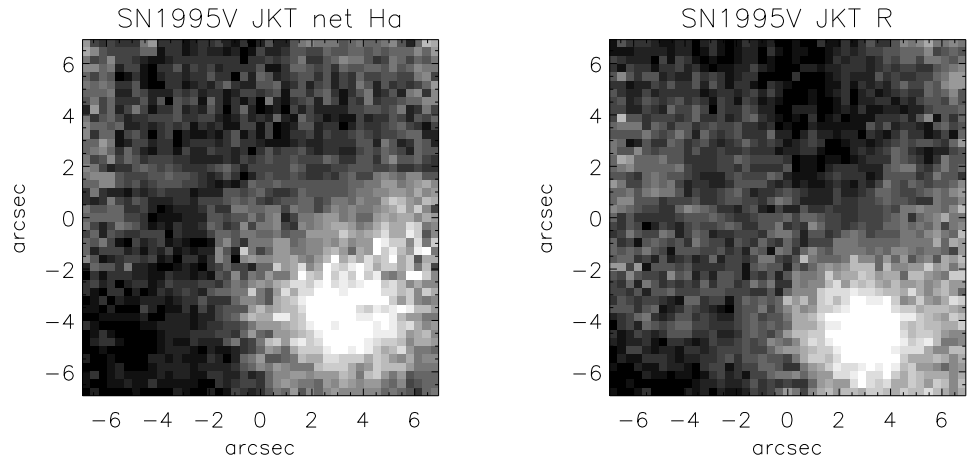

Figure A13. (left) JKT net Hα image (from James et al. 2004) showing the nebular environment of SN 1995V (at centre of image, Class 2). The 14×14 arcsec^2 field of view projects to 1×1 kpc^2 at the 14.4 Mpc distance of NGC 1087; (right) R-band image.

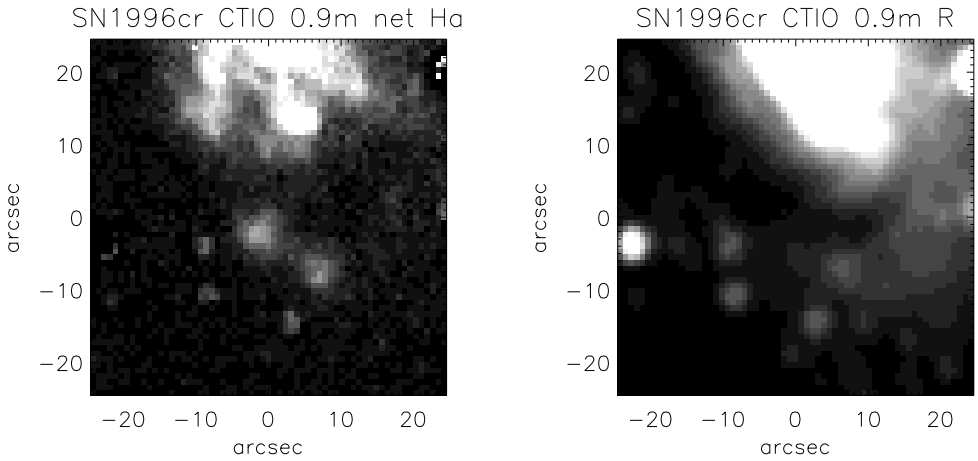

Figure A14. (left) CTIO 0.9m net Hα image (from Kennicutt et al. 2008) showing the nebular environment of SN 1996cr (at centre of image, Class 5). The 50×50 arcsec^2 field of view projects to 1×1 kpc^2 at the 4.21 Mpc distance of Circinus; (right) R-band image.

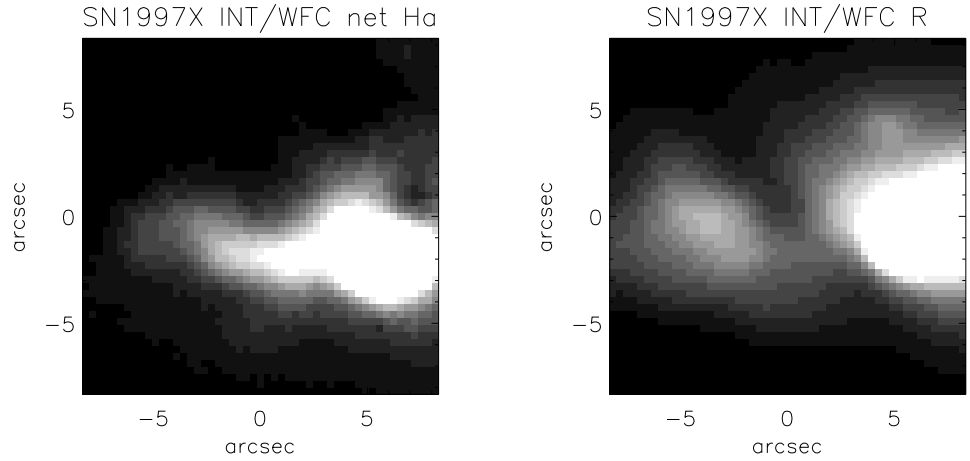

Figure A15. (left) INT/WFC net Hα image (from Anderson & James 2008) showing the nebular environment of SN 1997X (at centre of image, Class 3). The 17×17 arcsec^2 field of view projects to 1×1 kpc^2 at the 12 Mpc distance of NGC 4691; (right) R-band image.

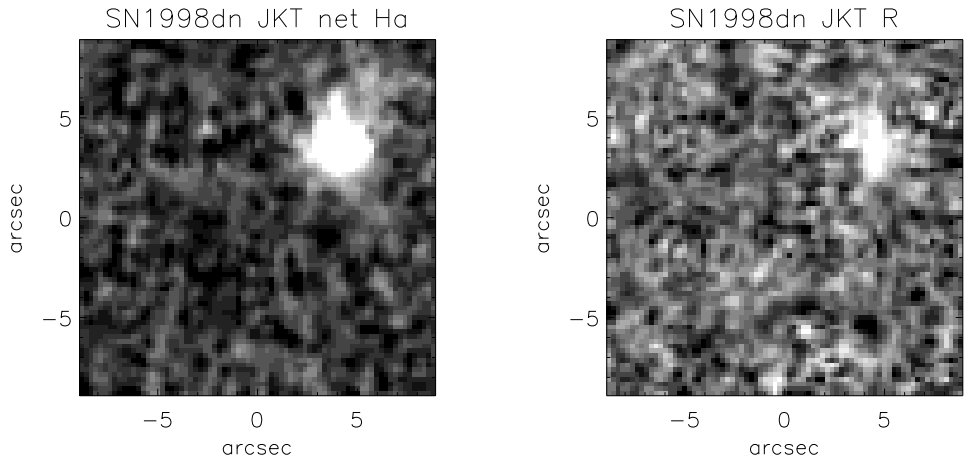

Figure A16. (left) JKT net Hα image (from Knapen et al. 2004) showing the nebular environment of SN 1998dn (at centre of image, Class 2). The 18×18 arcsec^2 field of view projects to 1×1 kpc^2 at the 12 Mpc distance of NGC 337A; (right) R-band image.

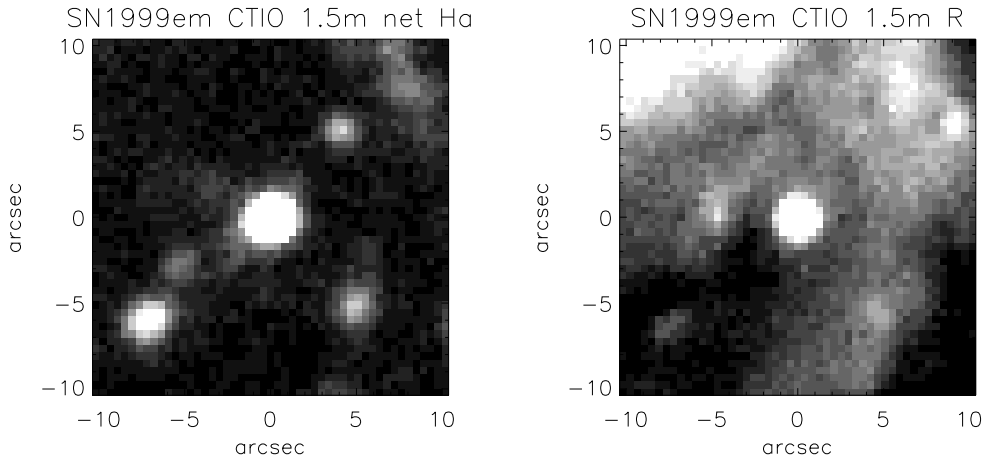

Figure A17. (left) CTIO 1.5m net Hα image from 26 Oct 2000 (Meurer et al. 2006) showing the nebular environment of SN 1999em (bright source at centre of image, Class 2). The 21×21 arcsec^2 field of view projects to 1×1 kpc^2 at the 9.77 Mpc distance of NGC 1637; (right) R-band image.

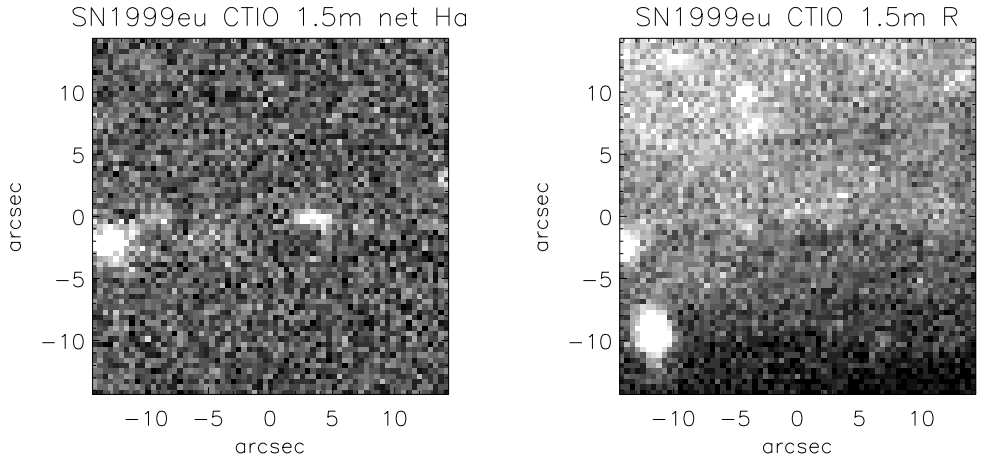

Figure A18. (left) CTIO 1.5m net Hα image (Kennicutt et al. 2003) showing the nebular environment of SN 1999eu (at centre of image, Class 2). The 29×29 arcsec^2 field of view projects to **2×2** kpc^2 at the 14.2 Mpc distance of NGC 1097; (right) R-band image.

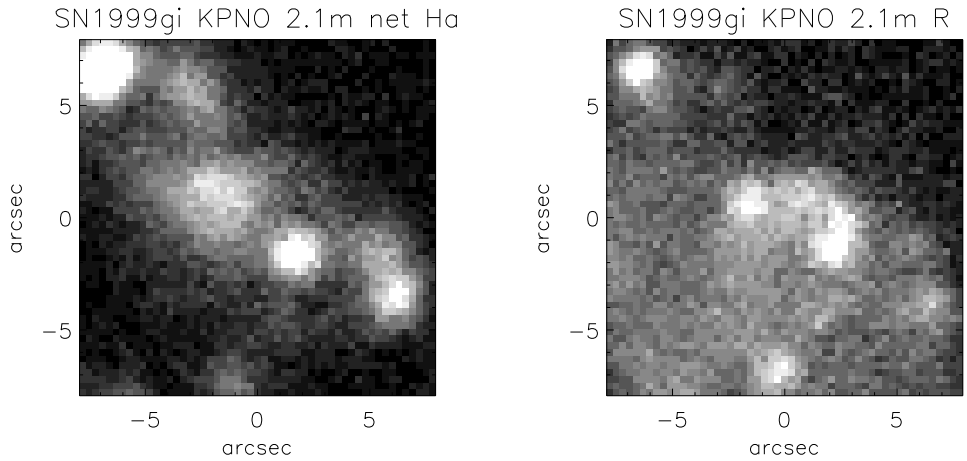

Figure A19. (left) KPNO 2.1m net Hα image (Kennicutt et al. 2003) showing the nebular environment of SN 1999gi (at centre of image, Class 5). The 16×16 arcsec^2 field of view projects to 1×1 kpc^2 at the 13 Mpc distance of NGC 3184; (right) R-band image.

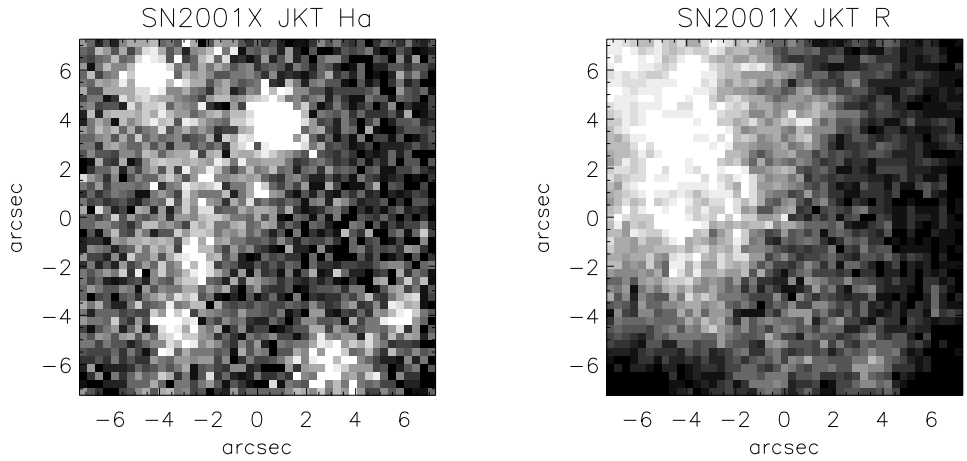

Figure A20. (left) JKT Hα image from Mar 1999 showing the nebular environment of SN 2001X (source at centre of image, Class 3). The 14.7×14.7 arcsec^2 field of view projects to 1×1 kpc^2 at the 14 Mpc distance of NGC 5921; (right) R-band image from Mar 2003.

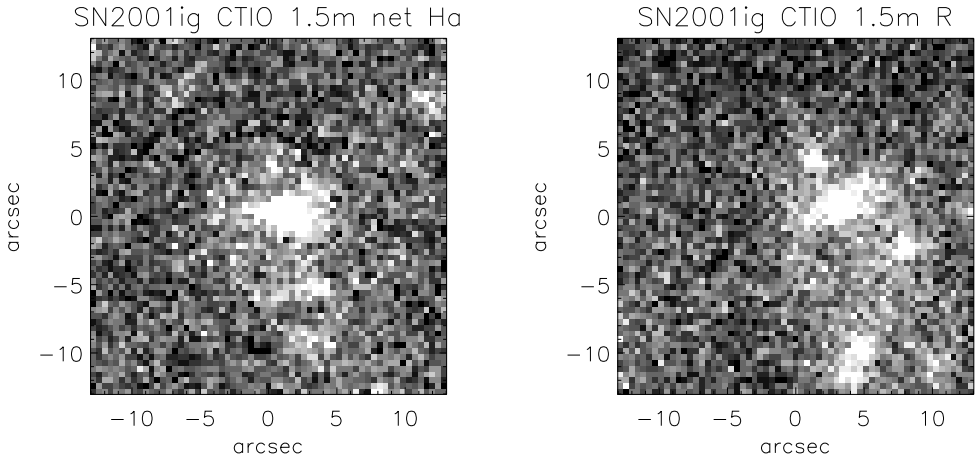

Figure A21. (left) CTIO 1.5m Hα imaging (Meurer et al. 2006) showing the nebular environment of SN 2001ig (source at centre of image, Class 4). The 16×16 arcsec^2 field of view projects to 1×1 kpc^2 at the 7.94 Mpc distance of NGC 7424; (right) R-band imaging.

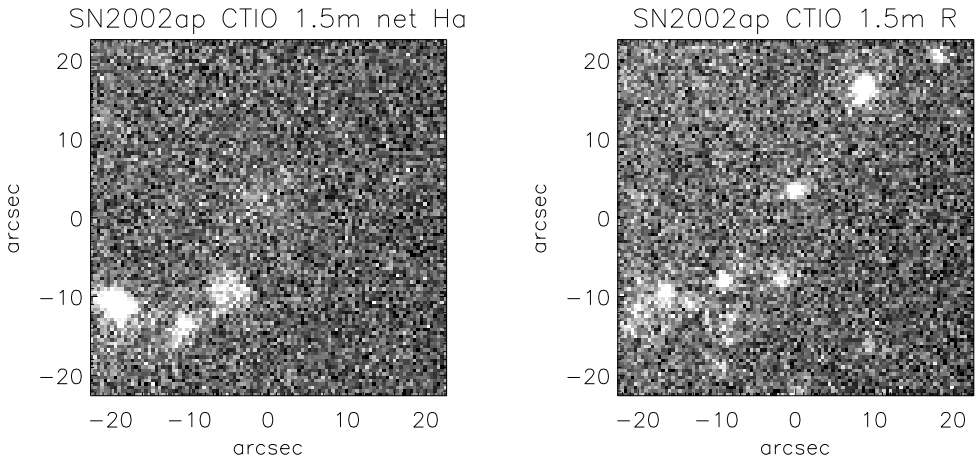

Figure A22. (left) CTIO 1.5m Hα imaging (Kennicutt et al. 2003) showing the nebular environment of SN 2002ap (source at centre of image, Class 2). The 46×46 arcsec^2 field of view projects to **2×2** kpc^2 at the 9 Mpc distance of M 74; (right) R-band imaging.

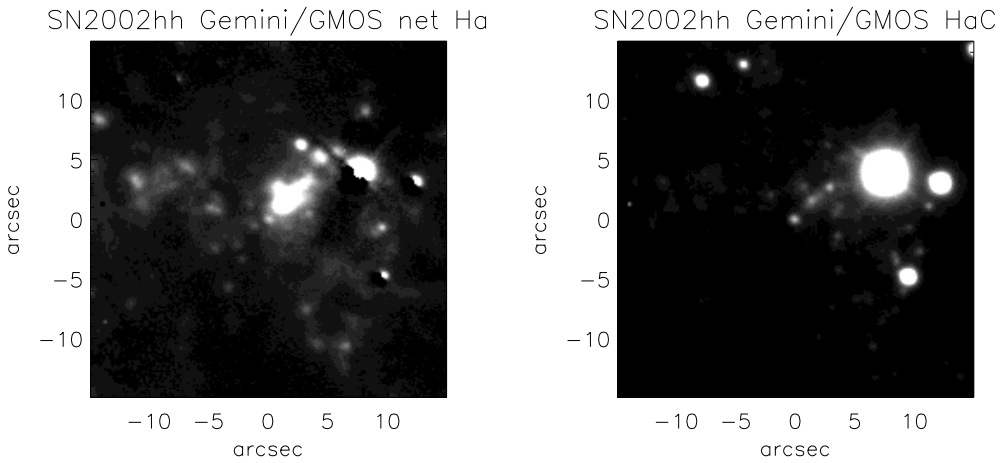

Figure A23. (left) Gemini/GMOS net Hα image (from GN-2009B-Q-4) showing nebular emission close to the position of SN 2002hh (at centre of image, Class 5). The 30×30 arcsec^2 field of view projects to 1×1 kpc^2 at the 7.0 Mpc distance of NGC 6946; (right) Continuum image (λ_c = 6620Å).

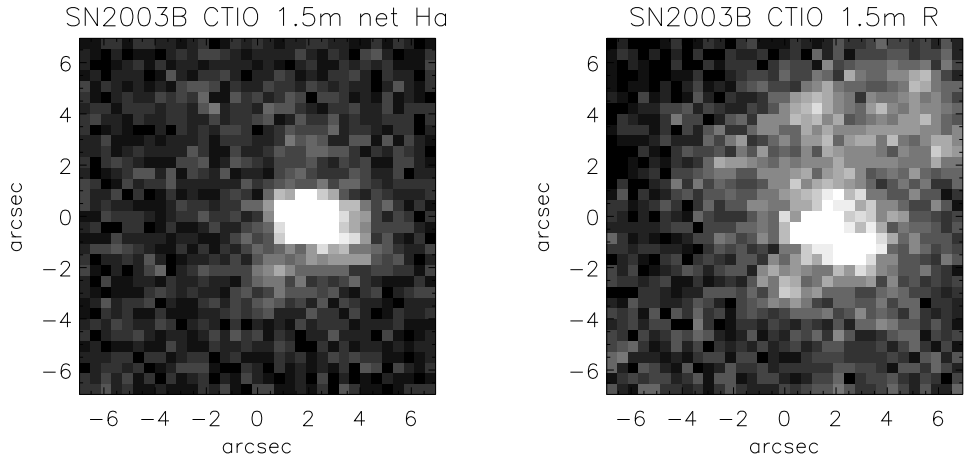

Figure A24. (left) CTIO 1.5m net Hα image (Kennicutt et al. 2003) showing the nebular environment of SN 2003B (at centre of image, Class 5). The 14.5×14.5 arcsec^2 field of view projects to 1×1 kpc^2 at the 14.2 Mpc distance of NGC 1097; (right) R-band image.

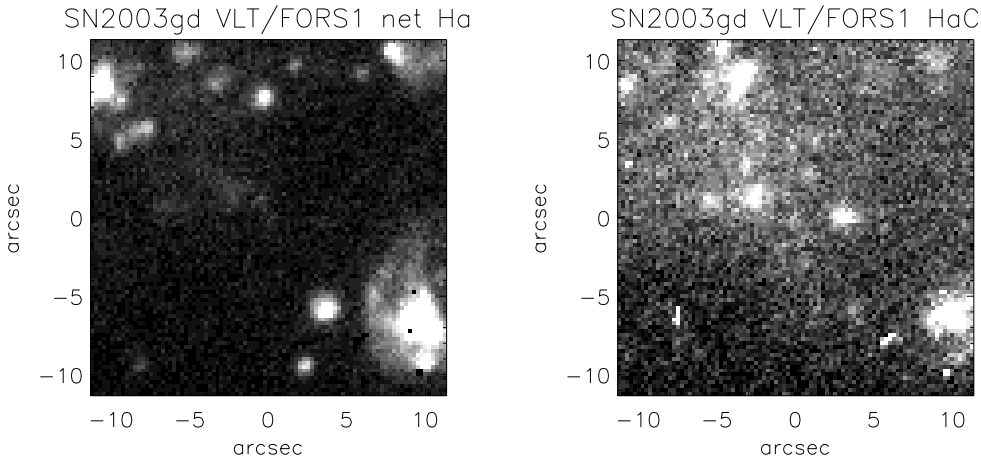

Figure A25. (left) VLT/FORS1 net Hα image showing the nebular environment of SN 2003gd (at centre of image, Class 2). The 23×23 arcsec^2 field of view projects to 1×1 kpc^2 at the 9.0 Mpc distance of M 74; (right) -band image.

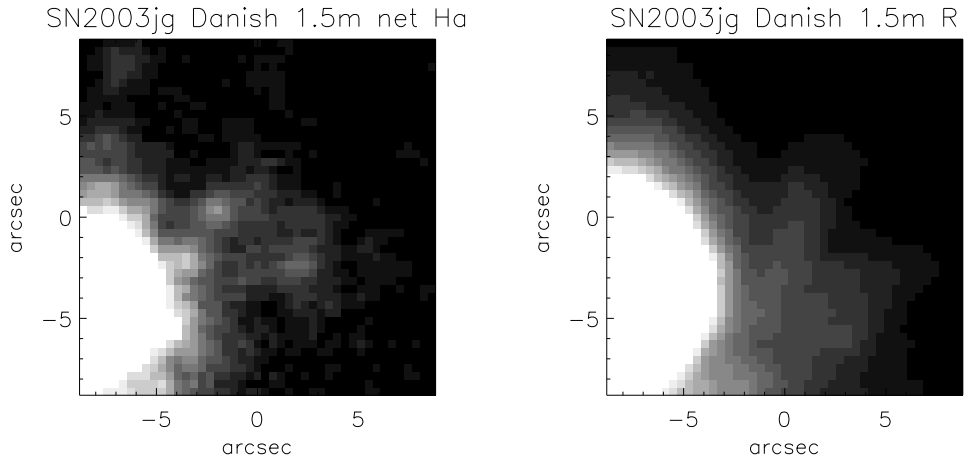

Figure A26. (left) Danish 1.5m net Hα image (from Larsen & Richtler 1999) showing the nebular environment of SN 2003jg (at centre of image, Class 2). The 18×18 arcsec^2 field of view projects to 1×1 kpc^2 at the 11.7 Mpc distance of NGC 2997; (right) R-band image.

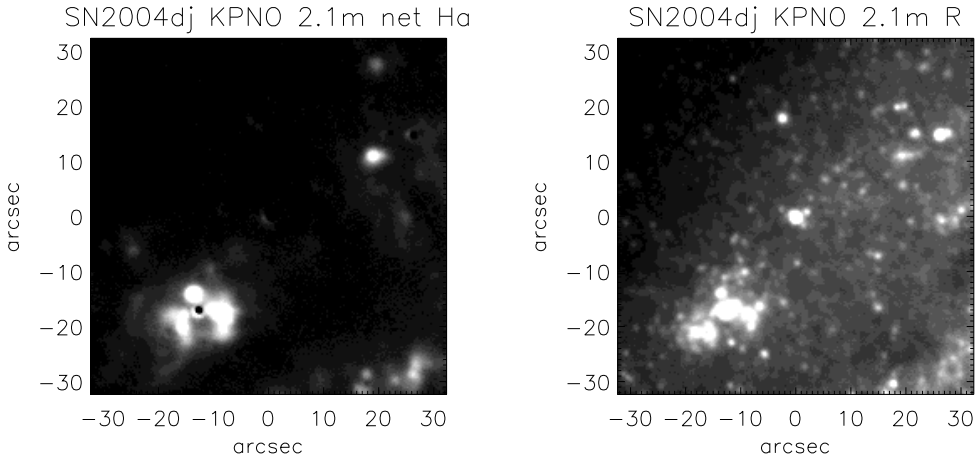

Figure A27. (left) 2.1m KPNO Hα image (from Kennicutt et al. 2003) showing the nebular environment of SN 2004dj (at centre of image, Class 1). The 65×65 arcsec^2 field of view projects to 1×1 kpc^2 at the 3.16 Mpc distance of NGC 2403; (right) R-band image.

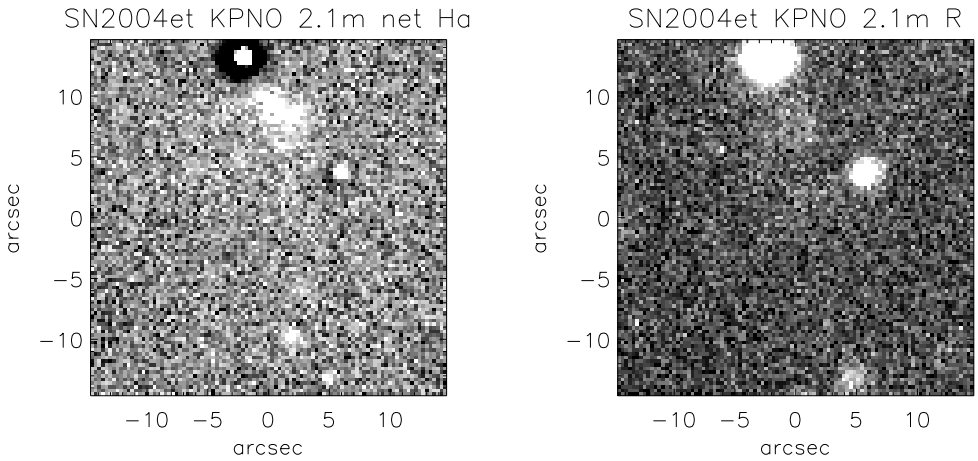

Figure A28. (left) 2.1m KPNO Hα image (from Kennicutt et al. 2003) showing the nebular environment of SN 2004et (at centre of image, Class 2). The 30×30 arcsec^2 field of view projects to 1×1 kpc^2 at the 7.0 Mpc distance of NGC 6946; (right) R-band image.

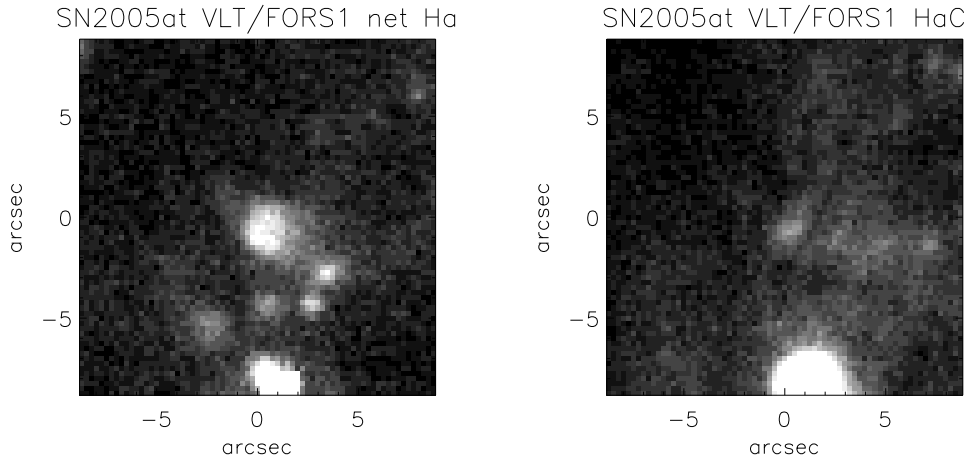

Figure A29. (left) VLT/FORS1 Hα image (081.B-0289(C), PI P.A. Crowther) showing the nebular environment of SN 2005at (at centre of image, Class 4). The 18×18 arcsec^2 field of view projects to 1×1 kpc^2 at the 11.6 Mpc distance of NGC 6744; (right) Continuum (λ_c = 6665Å) image.

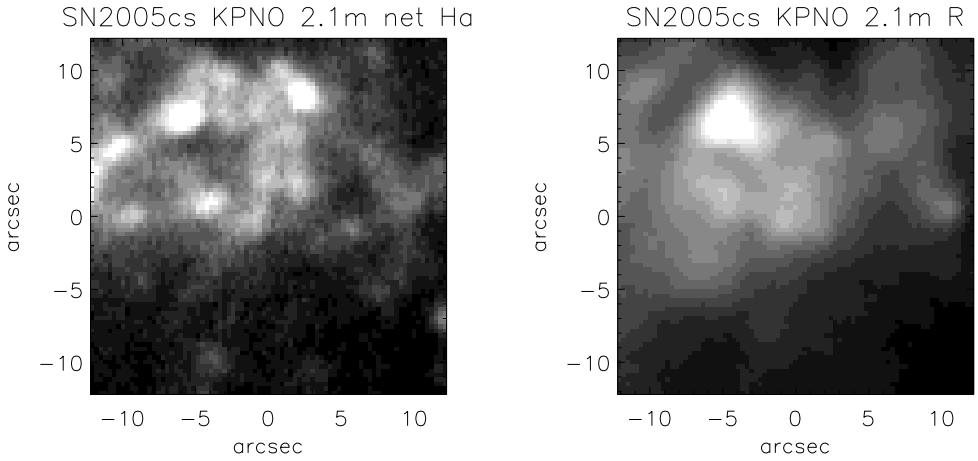

Figure A30. (left) KPNO 2.1m net Hα image (from Kennicutt et al. 2003) showing the nebular environment of SN 2005cs (at centre of image, Class 4). The 25×25 arcsec^2 field of view projects to 1×1 kpc^2 at the 8.4 Mpc distance of M 51a; (right) R-band image.

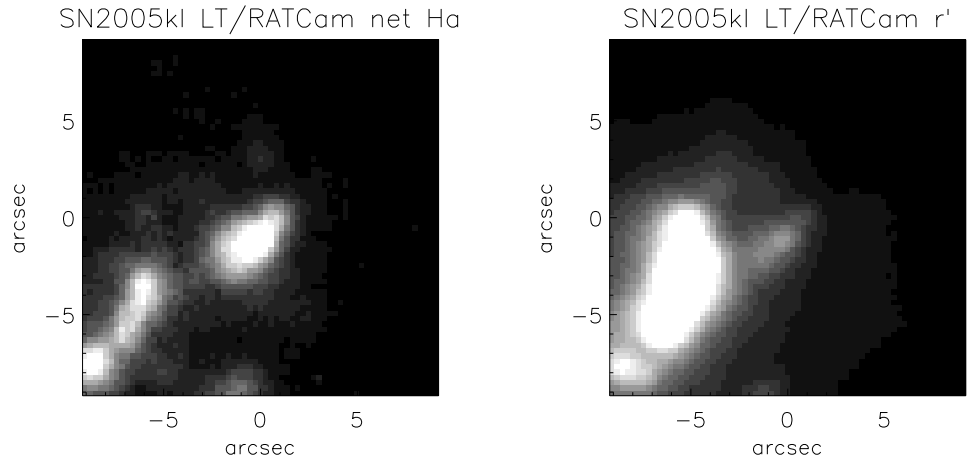

Figure A31. left) Liverpool Telescope RATCam net Hα image (from Anderson & James 2008) showing the nebular environment of SN 2005kl (at centre of image, Class 5). The 18×18 arcsec^2 field of view projects to 1×1 kpc^2 at the 11.2 Mpc distance of NGC 4369; (right) Sloan r′-band image.

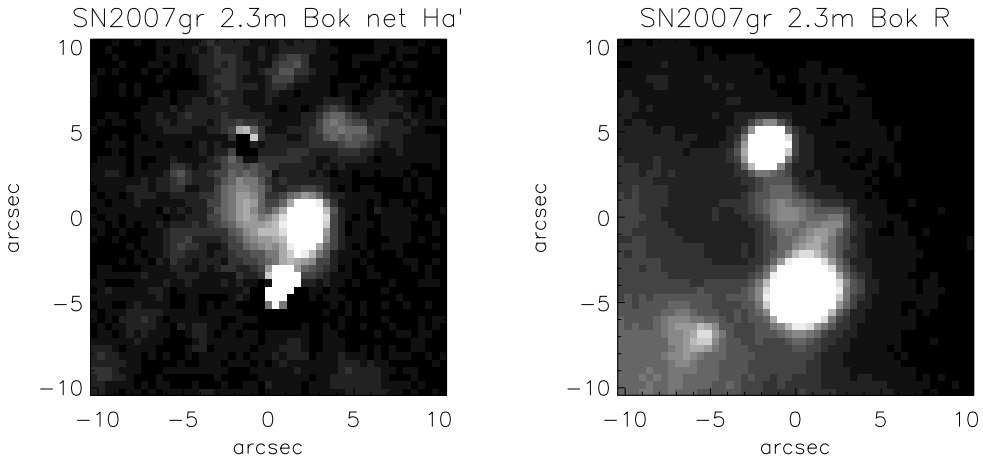

Figure A32. left) Bok 2.3m net Hα image (from Kennicutt et al. 2008) showing the nebular environment of SN 2007gr (at centre of image, Class 5). The 21×21 arcsec^2 field of view projects to 1×1 kpc^2 at the 9.86 Mpc distance of NGC 1058; (right) R-band image.

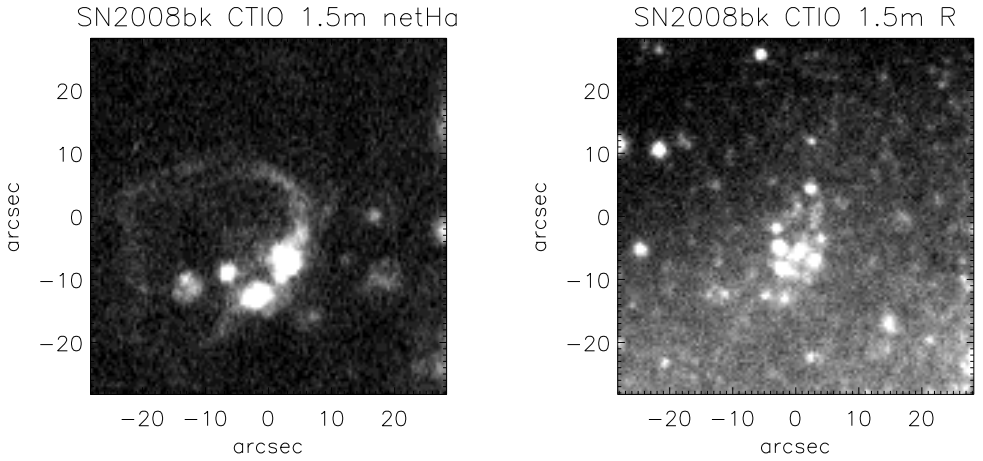

Figure A33. left) CTIO 1.5m net Hα image (from Kennicutt et al. 2003) showing the nebular environment of SN 2008bk (at centre of image, Class 2). The 57×57 arcsec^2 field of view projects to 1×1 kpc^2 at the 3.61 Mpc distance of NGC 7793; (right) R-band image.

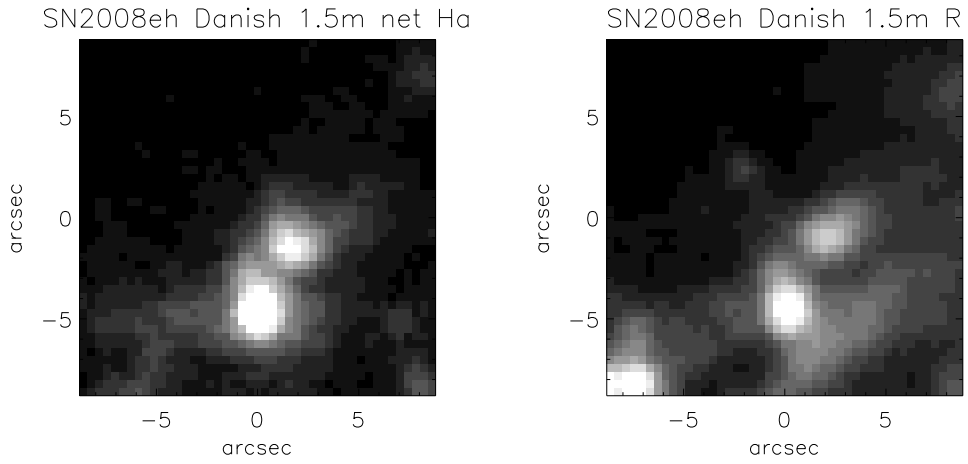

Figure A34. (left) Danish 1.5m net Hα image (from Larsen & Richtler 1999) showing the nebular environment of SN 2008eh (at centre of image, Class 5). The 18×18 arcsec^2 field of view projects to 1×1 kpc^2 at the 11.7 Mpc distance of NGC 2997; (right) R-band image.

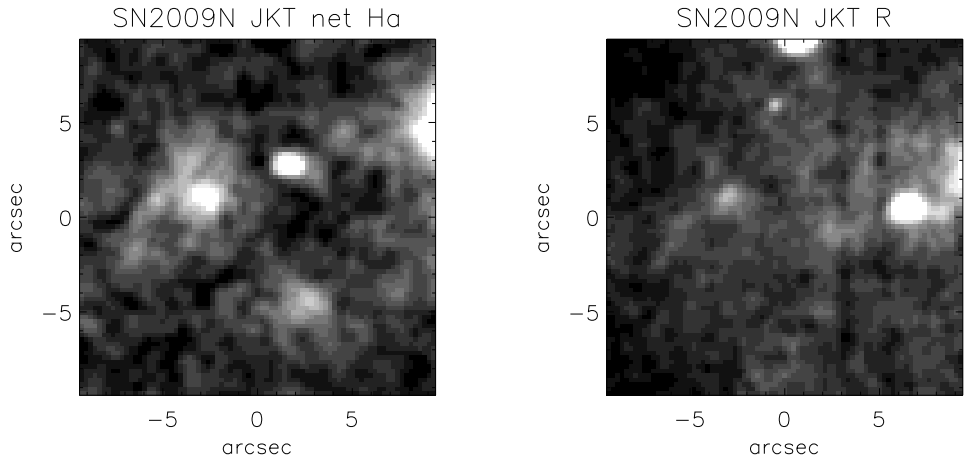

Figure A35. left) JKT net Hα image (from Knapen et al. 2004) showing the nebular environment of SN 2009N (at centre of image, Class 2). The 19×19 arcsec^2 field of view projects to 1×1 kpc^2 at the 11.0 Mpc distance of NGC 4487; (right) R-band image.

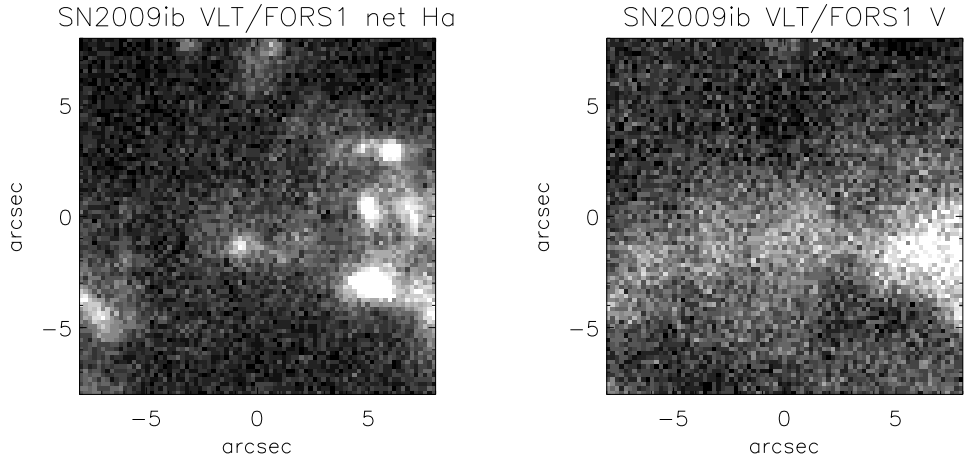

Figure A36. left) VLT/FORS1 net Hα image (from 075.D-0213(A)) showing the nebular environment of SN 2009ib (at centre of image, Class 2). The 16×16 arcsec^2 field of view projects to 1×1 kpc^2 at the 12.6 Mpc distance of NGC 1559; (right) V-band image.

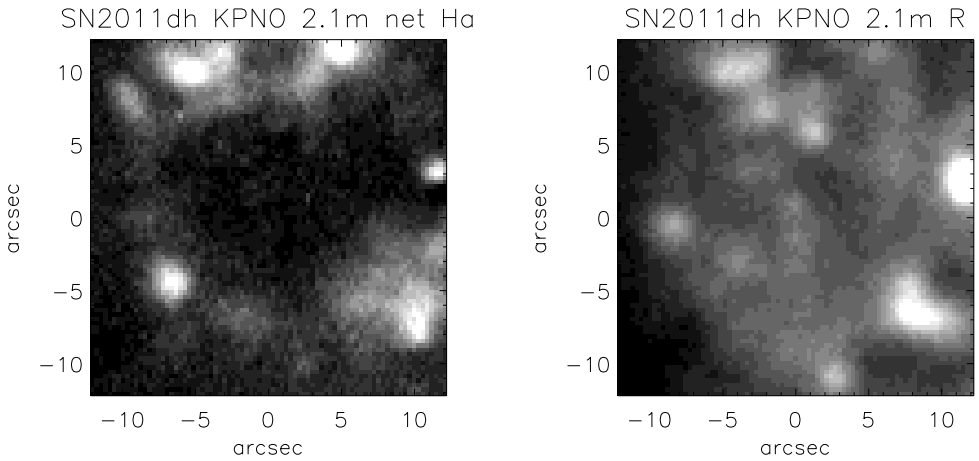

Figure A37. (left) KPNO 2.1m net Hα image (from Kennicutt et al. 2003) showing the nebular environment of SN 2011dh (at centre of image, Class 2). The 25×25 arcsec^2 field of view projects to 1×1 kpc^2 at the 8.39 Mpc distance of M 51a; (right) R-band image.

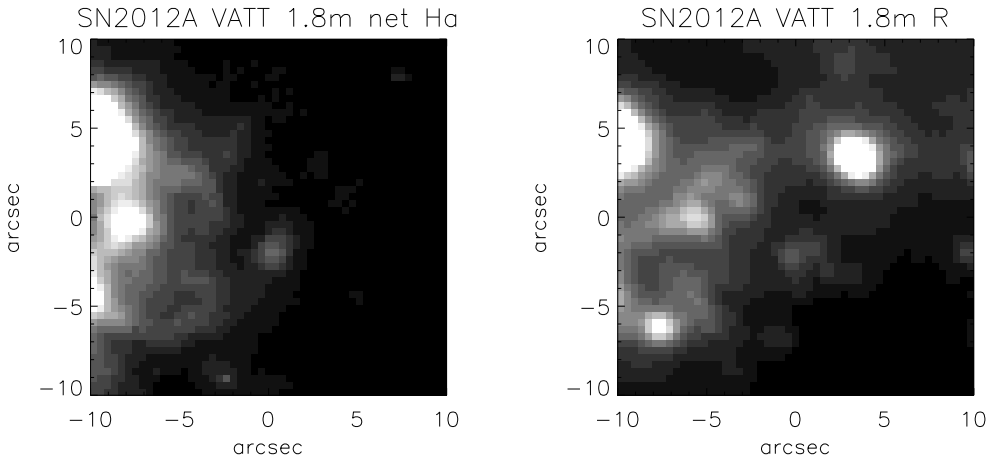

Figure A38. left) VATT 1.8m net Hα image (from Kennicutt et al. 2008) showing the nebular environment of SN 2012A (at centre of image, Class 4). The 20×20 arcsec^2 field of view projects to 1×1 kpc^2 at the 10.0 Mpc distance of NGC 3239; (right) R-band image.

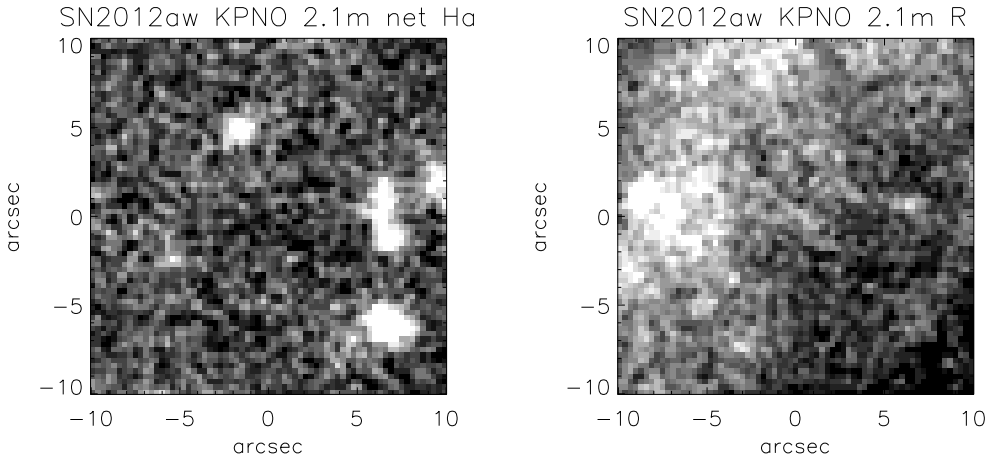

Figure A39. (left) KPNO 2.1m net Hα image (from Kennicutt et al. 2003) showing the nebular environment of SN 2012aw (at centre of image, Class 2). The 20×20 arcsec^2 field of view projects to 1×1 kpc^2 at the 10.0 Mpc distance of M 95; (right) R-band image.

APPENDIX B: CORE-COLLAPSE SNE LOCATED AT DISTANCES OF 15–20 MPC

Basic properties of ccSNe host galaxies located at distances of 15–20 Mpc (from Tully et al. 2009). Separate Tables are presented for low inclination (≤65°) hosts for which accurate ccSNe positions are known (Table B1) and high inclination hosts and ccSNe whose coordinates are imprecisely known (Table B2).

Table B1. Basic properties of host galaxies of ccSNe, drawn from RC3 or HyperLeda, for which EDD distances lie in the range 15–20 Mpc, restricted to low inclination (≤65°) hosts for which accurate ccSNe positions are known. SN imposter hosts are also omitted (e.g. SN 2003gm in NGC 5334, Smartt et al. 2009)

PGC	M	NGC	UGC	Type	cz (km s^{-1})	i	d (Mpc)			Ref	ccSNe
02081		157		SAB(rs)bc	1652	61.8	20.0			1	2009em
03572		337		SB(s)d	1648	50.6	19.5	±	1.6	1	2011dq
06826		701		SB(rs)c	1831	62.4	19.3	±	3.8	1	2004fc
09236		918	01888	SAB(rs)c?	1507	57.6	16.1	±	3.2	1	2009js
09846		991		SAB(rc)s	1532	28.1	17.3	±	1.1	1	1984L
10464		1084		SA(s)c	1407	49.9	17.3	±	1.1	1	1996an, 1998dl, 2009H
11479		1187		SB(r)c	1390	44.3	18.9	±	2.6	1	1982R, 2007Y
13179		1365		SB(s)b	1636	62.7	18.0	±	1.8	1	1983V, 2001du
14617		– ESO G420-G009 –		SB(s)c	1367	41.7	17.7	±	1.2	2	2003bg
14620		1536		SB(s)c pec?	1217	44.8	18.0	±	1.0	1	1997D
15850		1640		SB(r)b	1604	17.2	16.8	±	3.5	1	1990aj
29469			05460	SB(rs)d	1093	39.7	20.0			1	2011ht
31650		3310	05786	SAB(r)bc pec	993	16.1	20.0			1	1991N
32529		3423	05962	SA(s)cd	1011	32.1	17.0	±	2.5	1	2009ls
34767		3631	06360	SA(s)c	1156	34.7	18.0			1	*1964A*, *1965L*, 1996bu
36243		3810	06644	SA(rs)c	992	48.2	16.3	±	1.7	1	1997dq, 2000ew
37229		3938	06856	SA(s)c	809	14.1	17.1	±	0.8	1	*1961U*, 1964L, 2005ay
37290		3949	06869	SA(s)bc?	800	56.5	17.1	±	0.8	1	2000db
37306		3953	06870	SB(r)bc	1052	62.1	17.1	±	0.8	1	2006bp
37735			06983	SB(rs)cd	1082	37.4	17.1	±	0.8	1	1994P
37845		4030	06993	SA(s)bc	1465	47.1	19.5	±	1.5	1	2007aa
38068		4051	07030	SAB(rs)bc	700	30.2	17.1	±	0.8	1	*1983I*, 2003ie, 2010br
39578	99	4254	07345	SA(s)c	2407	20.1	1.8	±	0.8	1	*1967H*, *1972Q*, 1986I
40001	61	4303	07420	SAB(rs)bc	1566	18.1	17.6	±	0.9	1	*1926A*, 1961I, *1964F*, 1999gn, 2006ov, 2008in
40153	100	4321	07450	SAB(s)bc	1571	23.4	15.2	±	1.5	1	1979C
40745		4411B	07546	SAB(s)cd	1272	26.6	16.8	±	0.8	1	1992ad
41050		4451	07600	Sbc?	864	53.6	16.8	±	0.8	1	1985G
41746		4523	07713	SAB(s)m	262	25.1	16.8	±	0.8	1	1999gq
42833		4651	07901	SA(rs)c	788	49.5	16.8	±	0.8	1	1987K, 2006my
43321		4699		SAB(rs)b	1394	42.6	15.3	±	1.0	1	1983K
43972		4790		SB(rs)c?	1344	58.8	15.3	±	1.0	1	2012au
44797		4900	08116	SB(rs)c	960	19.0	15.6	±	1.0	1	1999br
45948		5033	08307	SA(s)c	875	64.6	18.5	±	1.1	1	1985L, 2001gd
52935		– Arp 261 –		IB(s)m pec	1856	58.8	20			1	1995N
58827		6207	10521	SA(s)c	852	64.7	18.1	±	2.1	1	2004A
59175		6221		SB(s)c	1499	50.9	15.6	±	1.7	1	1990W
70094		— IC 5267 —		SA0/a(s)	1712	48.4	18.7	±	1.6	1	2011hs

1: Tully et al. (2009), 2: NED (Virgo + GA + Shapley)

Table B2. Basic properties of host galaxies of ccSNe, drawn from RC3 or HyperLeda, for which EDD distances lie in the range 15–20 Mpc, restricted to high inclination (≥65°) hosts and ccSNe whose coordinates are imprecisely known (in italics). SN imposters are omitted.

PGC	M	NGC	UGC	Type	cz (km s^{-1})	i	d (Mpc)	Ref	ccSNe
09057		908		SA(s)c	1509	**65.1**	19.0 ± 1.6	1	1994ai
09354	—— Mk 1039 ——			Sc?	2111	**75.6**	19.2 ± 4.0	1	*1985S*
10065		1035		SA(s)c?	1241	**74.5**	17.3 ± 1.1	1	*1990E*
12007		1255		SAB(rs)bc	1686	58.8	20.0 ± 1.2	1	*1980O*
13586		1433		(R)SB(r)ab	1075	**67.4**	16.8 ± 1.0	1	1985P
13633			02813	Im?	1392	**76.6**	16.1 ± 1.5	1	2008fb
13727		1448		SAcd?	1168	**86.1**	16.8 ± 1.0	1	*1983S*, 2003hn
13985	– ESO G302-G014 –			IB(s)m	872	**73.6**	16.8 ± 1.0	1	2008jb
14123			02890	Sdm pec?	1155	**90**	16.1 ± 1.5	1	2009bw
19531		2280		SA(s)cd	1899	**66.2**	20.0 ± 1.4	l	2001fz
19579		2273B	03530	SB(rs)cd:	2101	**67.9**	17.9 ± 2.2	1	2011fd
36699		3877	06745	SA(s)c?	895	**83.2**	17.1 ± 0.8	1	1998S
37912	IC 755	4019	07001	SBb?	1524	**90**	16.8 ± 0.8	1	1999an
38302		4088	07081	SAB(rs)bc	757	**71.2**	17.1 ± 0.8	1	1991G, 2009dd
38580		4129		SB(s)ab?	1177	**90**	18.0 ± 3.8	1	2002E
38618		4136	07134	SAB(r)c	609	22	16.3 ± 0.9	1	*1941C*
38795		4157	07183	SAB(s)b?	774	**90**	17.1 ± 0.8	1	*1937A*, 2003J
39724		4274	07377	(R)SB(r)ab	930	**68**	16.3 ± 0.9	1	1999ev
39974		4302	07418	Sc?	1149	**90**	16.8 ± 0.8	1	1986E
40530	– IC 3311 –		07510	Sdm?	–122	**90**	20.0 ± 1.0	2	2004gk
41608	– IC 3476 –		07695	IB(s)m?	–169	51.2	16.8 ± 0.8	1	*1970A*
41789		4527	07721	SAB(s)bc	1736	**81.2**	17.6 ± 0.9	1	2004gn
42069		4568	07776	SA(rs)bc	2255	**67.5**	16.8 ± 0.8	1	1990B, 2004cc
42975		4666	07926	SABc:	1529	**69.6**	15.7 ± 2.9	1	*1965H*
43189		4688	07961	SB(s)cd	986	23.7	15.6 ± 1.0	1	*1966B*
43969		4809	08034	Im pec	915	**90**	15.6 ± 1.0	1	2011jm
53247		5775	09579	SBc?	1681	**83.2**	19.8 ± 1.0	1	1996ae
54117		5879	09753	SA(rs)bc?	772	**72.7**	15.5 ± 0.9	1	*1954C*
54470		5907	09801	SA(s)c?	667	**90**	17.2 ± 0.9	1	*1940A*

1: Tully et al. (2009), 2: Solanes et al. (2002)